# EXTRACELLULAR MATRIX PROTEIN LAMININ DRIVES MOTILITY IN GRANULOCYTE-MACROPHAGE PROGENITORS IN SINGLE-CELL CULTURE

by
Cassandra Greene

A thesis submitted to Johns Hopkins University in conformity with the requirements for the degree of Master of Science in Biotechnology

Baltimore, Maryland
August 2017

© 2017 Fluidigm Corporation. All rights reserved.

# i. Abstract

Single-cell culture is emerging as a powerful tool for transcriptomics with heterogeneous cell populations, but adequate *in vitro* extracellular matrix (ECM) conditions have yet to be determined for singulated culture of most cell types. In the absence of cell-to-cell signaling present in bulk culture, characterizing the effect of ECM proteins in single-cell culture is crucial to effective experimental design. In order to address this need and expand the capabilities of the Polaris™ system for single-cell culture, varied ECM proteins were applied for the first time to Polaris microfluidic cell culture integrated fluidic circuits (IFC). Granulocyte-macrophage progenitor cells (GMPs) purified from human cord blood were cultured on laminin-521, collagen 1, truncated vitronectin, fibronectin and unmodified PDMS. Laminin significantly increased cell motility relative to the other ECMs. Sequencing the cDNA libraries generated from these cells revealed differential gene expression for each ECM condition. Genes associated with pathways of motility driven by small Rho GTPases Rac, RhoA, and CDC42 were significantly overexpressed in cells cultured on laminin relative to cells cultured on PDMS. CD34 expression was also far overexpressed in the laminin-cultured cells, suggesting that in as little as 24 hours of single-cell culture, ECM may impact cell fate. This work demonstrates for the first time the application of diverse ECMs on Polaris, and exhibits its utility in performing single-cell studies.

*Readers and advisors: Dr. Chad Sanada, Dr. Kristina Obom, and Dr. Thomas Koval*

# ii. Acknowledgements

First, I would like to thank Dr. Chad Sanada for seeing this project through with me, despite the many logistical hurdles and technical challenges we faced along the way. If in the course of facing those challenges I have absorbed even a tiny fraction of your patience, tenacity, and composure, then I feel that I have succeeded.

I must express my gratitude to Dr. Anne Leyrat, who kindly encouraged me to begin this degree and go forward with this project – it has already made all the difference in the world. I must also bashfully thank my coworkers, friends, and family for supporting me and letting me complain more than they should have.

I am also extremely grateful to Fluidigm® for providing all of the technical and financial resources and that enabled this project to move forward.

By the time this document is formally submitted, my fiancé Dr. Jacob Chamoun will be my husband. I will save the full breadth of my feelings for my wedding vows – here, I will only say thank you. Thank you, thank you, thank you.

# iii. Table of Contents

**i. Abstract** ..... **i**

**ii. Acknowledgements** ..... **ii**

**iii. Table of Contents** ..... **iii**

**iv. List of Tables** ..... **v**

**v. List of Figures** ..... **vi**

**1. Introduction** ..... **1**

1.1. Granulocyte-macrophage progenitor cells ..... 1

1.2. The Polaris™ system ..... 2

1.3. Impact of ECM on pathways of motility ..... 4

**2. Materials and Methods** ..... **7**

2.1. Extracellular matrix modifications to Polaris ..... 7

2.2. Cell culture and FACS ..... 8

2.3. Polaris single-cell culture experiments ..... 9

2.4. mRNA Seq library preparation and sequencing ..... 10

**3. Results** ..... **12**

3.1. Extracellular matrix modifications pose a moderate risk to IFC function ..... 12

3.2. ECM performance in single-cell culture experiments with modified bead formulation is variable ..... 13

3.3. Laminin increases motility in single-cell and bulk culture ..... 14
3.4. Differentially expressed genes in single cells outline motility-related signaling pathways ..... 25
3.5. Differential gene expression results from MCSF dosing of single cells on Polaris ..... 20
**4. Discussion ..... 21**
4.1. Extracellular matrix and 4.5um bead loading can cause resistance to flow ..... 21
4.2. Culture of granulocyte-macrophage progenitors on Polaris successfully yields cDNA for sequencing ..... 22
4.3. Sequencing metrics and data normalization ..... 23
4.4. Gene expression analysis suggests small Rho GTPases drive motility ..... 25
4.5. Gene expression analysis is inconclusive regarding differentiation ..... 28
**5. Conclusion and Future Directions ..... 30**
**6. Tables ..... 32**
**7. Figures ..... 34**
**8. Appendices ..... 51**
**9. References ..... 63**
**10. Biography ..... 72**

# iv. List of Tables

**Table 1.** Summary of results for proof-of-concept ECM deposition on the Polaris system. ..... 32

**Table 2.** Polaris IFC run outcomes including bead packs, cell selection accuracy, cell retention during culture, and viability by DAPI following culture. Ideal Polaris IFC runs using model cell types such as K562s have approximately 46-48 single cells selected, 40 or more cells retained during culture, and at least 35 live cells following culture. ..... 32

**Table 3.** Sequencing metrics for samples 1, 2, and 3. Samples 1 and 2 were prepped and sequenced in a single library, whereas sample 3 was prepped and run separately. ..... 33

**Table 4.** Number of genes identified by ANOVA with $p < 0.05$ for sample 3 ..... 33

**Table 5.** Number of genes identified by ANOVA with $p < 0.05$ for samples 1 and 2. ..... 33

## v. List of Figures

**Figure 1.** Schematic of hematopoiesis.. ..... 34

**Figure 2.** The Polaris™ system ..... 34

**Figure 3.** Mechanism of cell motility ..... 35

**Figure 4.** Fibronectin deposition on Polaris ..... 36

**Figure 5.** Laminin deposition on Polaris ..... 37

**Figure 6.** Vitronectin and collagen deposition on Polaris. ..... 38

**Figure 7.** Matrigel deposition on Polaris ..... 39

**Figure 8.** Workflow for GMP experiments on Polaris ..... 40

**Figure 9.** Bead packs on Polaris ..... 40

**Figure 10.** Motility during single-cell culture on Polaris. ..... 41

**Figure 11.** Bulk-cultured GMPs on different ECMs have different densities ..... 42

**Figure 12.** PCA and tSNE for Sample 3 GMPs cultured on Polaris ..... 43

**Figure 13.** Fold-difference in expression of genes comprising LFA-1 and VLA-5 in sample 3 GMPs. ..... 44

**Figure 14.** Principal component analysis for GMP samples 1 and 2 ..... 45

**Figure 15.** Hierarchical clustering of cells cultured on laminin and PDMS for Samples 1 and 2 46

**Figure 16.** Motility of GMP subgroups during single-cell culture ..... 47

**Figure 17.** Overexpression of genes coding for the Arp2/3 complex ..... 47

**Figure 18. Differential expression of genes of interest in GMP Samples 1 and 2**. ..... 48

**Figure 19.** ECM accumulation on downstream side of bead packs. ..... 49

**Figure 20.** Small Rho GTPases CDC42, Rac, and RhoA drive motility in a complex network of interactions. ..... 50

# 1. Introduction

## 1.1. Granulocyte-macrophage progenitor cells

Hematopoietic stem cells (HSCs) are a type of adult stem cell that give rise to all blood cell lineages, including lymphocytes, red blood cells, macrophages, and dendritic cells (1, 2). HSCs reside in the bone marrow in a niche composed of specialized cells and scaffolds that curate the precise conditions required to balance HSC differentiation and self-renewal (1, 3). In order to maintain their numbers, HSCs may divide symmetrically and produce two identical daughter cells with the same stemness and potential as the original cell. Conversely, in asymmetrical division, one daughter cell is identical to the original cell in stemness and the second daughter cell progresses towards a mature cell fate. To produce mature cells of a given type – for example, lymphocytes, red blood cells, or macrophages – daughter cells generated by dividing HSCs are exposed to signals that induce maturation into the required cell fate, often undergoing several rounds of division and intermediate stages of progenitors before reaching their final identity (1, 2, 4). Imbalances in this process can cause disease, including leukemias (in which excessive self-renewal causes an excess of immune cells) and anemias (in which a deficit of erythrocytes occurs due to lack of production from progenitors) (1-4). The hematopoietic niche maintains a delicate balance by cradling HSCs in an environment that provides a precise combination of inter-cell signaling and cues from the extracellular matrix.

One pathway of HSC differentiation is to the common myeloid progenitor (CMP) and then to granulocyte-macrophage progenitor (GMP), as illustrated in **Figure 1**. GMPs may then give rise to granulocytes including neutrophils, eosinophils, basophils, and monocytes,

which may further differentiate into macrophages (1, 5). GMPs are one of several subtypes of HSCs that have been well-characterized as expressing very particular surface markers. These markers may be used in fluorescence-activated cell sorting (FACS) to obtain a pure population of those cells for use in experimentation (5-7). However, even within a nominally pure population of GMPs some heterogeneity exists with regards to lineage potential, and that heterogeneity is poorly understood at present (8). There is also good deal of ambiguity in how exactly lineages converge, diverge, and are related to each other, or when cell fate decisions that impact downstream differentiation pathways are truly made. For example, there is conflicting evidence as to whether the monocyte/macrophage and granulocyte lineages downstream of GMPs bifurcate before or after the GMP stage (6, 9). Understanding these pathways will be key in increasing our general mastery of hematopoietic stem cell handling in the lab towards the goal of addressing diseases that arise from differentiation-related dysfunction.

Due to their relative abundance in umbilical cord blood, well-defined surface marker profile, and relatively limited potential (and therefore limited fate-related heterogeneity relative to upstream populations), GMPs are a good candidate for *in vitro* studies. They are also very sensitive to their niche *in vivo*, suggesting that they may yield significant results in studies concerned with optimizing *in vitro* culture conditions.

### 1.2. The Polaris™ system

Polaris is a benchtop instrument produced by Fluidigm Corporation that performs automated single-cell handling. As described in **Figure 2**, single cells are selected into

capture sites where they can be cultured for up to 24 hours with integrated imaging, and then processed to generate single-cell cDNA libraries. These cDNA libraries are produced by lysing the cells, reverse transcribing the cell's RNA into cDNA, and then amplifying the DNA – this process is called RT-PCR. All of these activities are carried out in an integrated fluidic circuit (IFC), a disposable microfluidic chip designed for manipulating small volumes of liquid in a precise manner (10). The resulting cDNA libraries present a snapshot of the genes being expressed by the cell at the time of lysis.

Single-cell work, such as that which may be performed using Polaris, is a useful tool for researchers because single-cell biology can provide unambiguous results when dealing with a heterogeneous cell population. Processing bulk samples of cells for sequencing may mask gene expression patterns due to group averaging and differences in the relative frequency of transcripts present in the bulk sample (11-13). Therefore, in order to gain higher-resolution data than can be obtained from cells processed in a large pool, researchers may choose to investigate single-cell gene culture and expression analysis. "Micro-heterogeneity," that is, heterogeneity within a nominally pure population of cells, is especially a challenge in HSC studies. HSCs are diverse not only in stochastic gene expression variations which affect any cell type, but also in their fate (12-14). While our understanding of HSC fate determination is still evolving, there is evidence that even in a progenitor state some cells may be pre-committed to one fate or another, or could be truly bi-potent. For example, as described in the previous section, a GMP could be pre-committed to a downstream fate despite appearing to be part of a carefully purified GMP population (6, 9). Such pre-determination is undetectable in bulk without growing out the cells into mature colonies and subsequently determining the phenotype or genotype of those more differentiated cells (14). There may

also be unidentified transitional states between known stages of hematopoiesis that are presently invisible due to the limitations of bulk studies (12, 13).

Single-cell culture is fundamentally different from bulk culture because in single-cell culture, the cell-cell signaling that normally occurs in bulk culture is absent (15). Mammalian cell culture often requires treatment of culture surfaces with extracellular matrix (ECM) proteins in order to promote optimal cell health and growth; this is especially true for HSCs. However, different ECMs may also have effects on cell fate and phenotype (3, 15-18). Presently, the only ECM options for Polaris are either the untreated polydimethylsiloxane (PDMS) that comprises the Polaris IFCs, or PDMS treated with fibronectin at a concentration of 25ng/uL. The range of applications of the system would increase significantly if compatibility were confirmed for a greater variety of ECMs. Due to the small microfluidic features of the Polaris IFC and the tendency of proteins to form aggregates, the introduction of untested ECMs may cause clogging or interfere with the RT-PCR reactions that are carried out on-IFC. Thus careful testing is required in order to vet new ECMs on Polaris, and must be pursued in order to make Polaris a more impactful research tool.

### 1.3. Impact of ECM on pathways of cellular motility

One of the many ways in which ECMs can affect cell culture is by influencing cell motility. ECM proteins contain ligands that interact with cell membrane molecules such as integrins, which triggers complex and diverse signaling cascades that result in motility. The essential steps of canonical “mesenchymal” cell motility are extension of the lamellopodium and filopodia, adhesion formation, and finally contraction of the cell that pulls it forward

(**Figure 3**) (19-21). Rho-family small GTPases including CDC42, Rac, and Rho are signaling hubs for all three steps, influencing the balance between protrusion via actin polymerization, contraction via myosin II activity, and disassembly of old adhesions (22).

Together, Rho GTPases and myosin II cause a sort of treadmilling of adhesions at the leading edge of the cell, meaning they are formed and disassembled at a roughly equivalent rate in different areas of the cell in such a way that the cell shifts forward (23, 24). Motility is initiated when an extracellular cue induces the cell to extend towards the cue via actin polymerization, which can occur either by broad lamellopodia or spiked filopodia structures (25). At the site of these protrusions, the actin skeleton is tethered to the extracellular components by adhesions that allow the cell to shift forward via actomyosin contraction. The formation of these adhesions influences cytoskeletal rearrangement and conversely, cytoskeletal changes influence the formation of new adhesions and the disassembly of older adhesions at the rear pole of the cell (24, 26). As actin polymerizes at the leading (a.k.a. barbed or "plus") edge, actin filament disassembly at the rear pointed ("minus") edge maintains filamentous and monomeric actin in a steady state, which is another form of treadmilling. Lamellar actin incorporated into the filament undergoes retrograde flow relative to the leading edge of the cell due to polymerization at the leading edge (barbed edge) and due to contraction driven by myosin. Adhesions are crucial in providing an anchor, or clutch, to this retrograde flow to allow protrusion to continue. The efficiency of this clutch to resist slippage (i.e. moving backward at a rate different from retrograde actin movement) and the exact pathways involved in motility differ between cell types and are therefore likely regulated (19, 20, 24).

This work explores the possibility of observing such regulations that govern motility pathways, which are inherently challenging to observe due to their transient and dynamic nature (14, 19). Human hematopoietic stem cells (HSCs) are a useful model cell for this work since they are sensitive to their niche in vivo (2, 16, 27). ECM proteins including laminin, collagen, and fibronectin have been observed to affect *in vitro* culture of HSCs, including their motility and differentiation (3, 4, 18). However, the degree to which single-cell culture on diverse ECMs recapitulates these effects has barely begun to be addressed by the scientific community (3).

As single-cell studies become increasingly prevalent, understanding these factors becomes increasingly important (12, 14). It is therefore imperative that we begin to investigate exactly which mechanisms of motility result from modifications to the *in vitro* culture environment. We hypothesize that choice of ECM in single-cell culture of GMPs produces differential gene expression that could potentially impact diverse cell functions including cell fate. In the work presented here, that hypothesis is addressed through novel single-cell culture experiments using the Polaris system. Singulated GMPs were cultured for 24 hours on Polaris IFCs whose culture chambers were coated with diverse ECMs. The cells were lysed, processed to generate single-cell cDNA libraries, and sequenced. This workflow enabled the determination of which genes are differentially expressed in GMPs as a result of culture on different ECMs, and what degree of heterogeneity is present between and within samples.

# 2. Materials and Methods

## 2.1. Extracellular matrix modifications to Polaris

Collagen from human placenta and bovine fibronectin were obtained from Sigma Aldrich, and hESC-qualified mouse matrigel was obtained from VWR. Recombinant human truncated vitronectin, recombinant human laminin-521, and SimplyBlue SafeStain were obtained from ThermoFisher. Laminin and Fibronectin HiLyte-Fluor488 were obtained from Cytoskeleton, Inc.

To demonstrate that increasing concentrations of ECM proteins produce increasing degrees of deposition, the scripts that orchestrate the priming step in the Polaris workflow were modified to enable customized ECM deposition. The modified scripts enabled the use of 6 inlets for ECM loading on a single IFC. Fluorescently labeled laminin and fibronectin at 6 concentrations ranging from 0 to 100 ng/ul were thus deposited onto two Polaris IFCs while maintaining all other typical aspects of the priming step. The IFCs were then imaged via fluorescence microscopy (Leica, 20X magnification) and the images were analyzed in ImageJ to determine fluorescence intensity for each ECM condition. For collagen, the native fluorescence of collagen in CY5 was measured following priming. For vitronectin, a secondary stain using Gibco SimplyBlue SafeStain was applied and then washed and imaged in CY5. The same secondary stain was attempted for matrigel, which was applied in dilutions ranging from 1:100 to 1:20.

## 2.2. Cell culture and FACS

Frozen human CD34+ cord blood cells from pooled donors, StemSpan SFEM II media, and StemSpan CC100 supplement were obtained from StemCell Technologies. Recombinant human macrophage colony stimulating factor (MCSF) from PeproTech was spiked into an aliquot of the prepared media at a concentration of 25 ng/uL. Surface marker antibodies for FACS sorting were obtained from Biolegend and BD Biosciences (Supplementary Tables 1 and 2). FACS was performed using a Sony LE-SH800 Series cell sorter, software version 1.5.1, with four lasers (405, 488, 562, and 633nm) that allows simultaneous detection of up to six colors.

Cell culture, staining, and sorting was performed by Dr. Chad Sanada. Cells were thawed and incubated for 24 hours, then stained and FACS sorted to obtain a population of granulocyte-macrophage progenitor (GMP) cells (**Supplementary Figure 1**). Ninety-six well plates were prepared with each ECM of interest by incubating with 100uL of 50 ng/uL ECM for 2 hours at room temperature, aspirating the ECM solution, and then washing three times with 100uL PBS+/+. Prepared plates were stored at 4C overnight with 100uL prepared media with or without MCSF, ready for FACS sorting. The following day bulk sorts of 4000 cells were sorted into ECM-treated wells containing media with and without MCSF to use as tube controls (Supplementary Tables 3 and 4). The remainder of the cells were sorted into a 12-well plate for use on Polaris. All plates were cultured at 37C for 24 hours. After 24 hours of culture, the 12-well plate contents were used for Polaris experiments while the wells containing 4000 bulk cells per well were imaged (Leica, 10X magnification), and processed

for RT-PCR with the same Clontech chemistry as on the Polaris IFC. A calibration plate was also run using spare cells to confirm the single cell and well sorting efficiency of the sorter (**Supplementary Table 5**).

This workflow was performed with three different lots of pooled cord blood – sample 3 was used for the testing of all ECMs, and samples 1 and 2 were tested only on laminin and untreated PDMS.

### 2.3. Polaris single-cell culture experiments

For cord blood sample 3, five Polaris IFCs were primed according to the Polaris user guide. A different ECM was loaded onto each IFC: 50ng/uL collagen, laminin, vitronectin, and fibronectin were loaded using the "adherent prime" option in the user interface, and one IFC was prepared with untreated PDMS ("suspension prime"). For cord blood samples 1 and 2, two Polaris IFCs were prepared with untreated PDMS and four were prepared with laminin-coated PDMS. These IFCs were divided evenly between samples 1 and 2 – that is, both samples 1 and 2 were run on one IFC with untreated PDMS and two with laminin.

After 24 hours of culture, the cells from the 12-well plate described in the previous section were stained with 0.1uM Calcein AM and 0.5uM Cell Tracker Orange (Life Technologies) for 30 minutes at room temperature, washed once by centrifuging at 200xg for 10 minutes then removing the supernatant and resuspending in FACS sorting buffer (HBSS + 2% FBS + 20mM HEPES + 2mM EDTA + 1mM Pyruvate + 0.1% F68 Pleuronic), and loaded onto Polaris IFCs. Single cells that were positive in both yellow and green channels

were captured on IFC and dosed for 24 hours with prepared media. 25% of the capture sites on each IFC were dosed with prepared media + MCSF for 24 hours. All cells were then stained with DAPI and imaged via fluorescence microscopy to assess live/dead status prior to proceeding with lysis, RT, and PCR on IFC. ArrayControl RNA spikes 1, 4, and 7 (Thermo Fisher) were included in the lysis mixture as a control at 1/100 dilution relative to the concentration specified in the Polaris User Guide and Protocol.

### 2.4. mRNA seq library generation and sequencing

Generation of cDNA from cell lysate was performed using Clontech's SMARTer Ultra Low RNA Kit for Illumina Sequencing and Advantage 2 PCR kit both on IFC and in tube according to the Polaris User Guide and Protocol. cDNA was quantified by Quant-iT Picogreen dsDNA assay (Thermo Fisher) prior to Illumina Nextera XT library prep. The pooled library was quantified by Bioanalyzer and Qubit prior to sequencing. Sequencing was performed on an Illumina NextSeq instrument using 300 cycle High-Output v2 kits with 150bp paired end reads. The FASTQ files generated by sequencing were processed using Fluidigm® internal data analysis pipeline which utilizes TopHat and Cufflinks for mapping to RefSeq. Subsequent gene expression analysis was performed using the Singular™ Analysis Toolset in R software, a package created and distributed by Fluidigm ®, using data normalized to TPM (transcripts per million). Determination of outliers to be omitted from the analysis, unsupervised hierarchical clustering (HC), PCA plots, and tSNE analysis were performed using the Singular Analysis Toolset for R. Sample groups were defined based on the initial unsupervised HC for subsequent ANOVA and PCA/tSNE/HC figure generation.

Gene ontology was analyzed using the PANTHER classification system (28-30). Wherever p-values are used in this analysis, they are for two-tailed t-tests with unequal variances. Standard error of the mean (SEM), when used, is defined as the standard deviation divided by the square root of the number of replicates.

# 3. Results

### 3.1.Extracellular matrix modifications pose a moderate risk to IFC function

The very first step in the Polaris workflow is to prime the IFC, which includes first depositing ECM on the surface of the capture/culture chamber, and then loading a solution of 10um polystyrene beads into the capture/culture chamber. These beads act as a fine sieve to catch cells as they are selected into the capture chamber while still allowing the flow of reagents past the cell. The sieve created by the beads is prone to clogging when reagents containing particulates are flowed through the chambers. The goal of the first set of experiments was to determine concentrations for ECM deposition in Polaris chambers that achieve a balance between effective deposition and minimal risk of IFC clogging.

To assess the compatibility of each ECM with the existing priming procedure, six concentrations of a given ECM were flowed onto each IFC during an otherwise normal Prime step. For fibronectin, fluorescence correlated with the concentration of fibronectin up until 50ng/uL. At 100ng/uL the fluorescence intensity as measured in ImageJ decreased, indicating possible quenching, clogging, saturation of the deposition surface, or the fibronectin falling out of solution (**Figure 4A**). The visible particulates at 100ng/uL corroborate the latter (**Figure 4B**, **C**). Note the dim capture chamber (sixth from the right, **Figure 2C**) indicating a probable clog on the IFC inhibiting the flow of reagents through the capture site, suggesting that 100ng/uL fibronectin is too concentrated to safely be used on the IFC.

Similarly, laminin concentration correlated with fluorescence intensity, with particulates visible at 100ng/uL (**Figure 5**). However, the drop-off in fluorescence intensity was not observed in this case.

Vitronectin and collagen were also deposited on IFCs to assess clogging and deposition. Although less quantitatively robust in nature due to lower signal to background ratios, these methods also demonstrated the same trend of increasing fluorescence with increasing ECM concentration (**Figure 6**). Both also demonstrated clogging above 50ng/uL.

The deposition of matrigel was also attempted, but as expected this caused clogs at every dilution factor used, ranging from 1:100 to 1:20. Beads only successfully loaded in the negative control chambers indicating severe clogging elsewhere (**Figure 7**). The results for proof-of-concept ECM deposition are summarized in **Table 1**.

### 3.2.ECM performance in single-cell culture experiments with modified bead formulation is variable

Following the optimization described in the previous section, each ECM was tested at 50 ng/uL in a single-cell culture experiment on Polaris using FACS-purified GMPs; this workflow is summarized in **Figure 8**.

In the cell-based experiments, mixture of 10um and 4.5um beads was used in place of the standard 10um beads (used in the proof of principle experiments) to create a finer sieve in the cell capture chambers to increase cell retention rates. The 4.5um beads had the unexpected and previously unobserved effect of reducing the overall number of beads on IFC, which is termed “underloading.” Underloading leads to instability of the bead pack during cell

selection and culture, causing lower capture and retention rates of small cells. Figure 9 provides examples of normal and underloaded beads.

For fibronectin, vitronectin, and collagen, it was also observed that there was some resistance to flow during cell selection that decreased capture accuracy and efficiency, resulting in some empty sites or multiple cells in a single site. It is possible that the 4.5um beads intrinsically cause some resistance to flow, but this effect seems to vary from experiment to experiment. The underpacking, flow resistance, and cell selection, retention, and viability metrics for all experiments are summarized in Table 2.

In the collagen IFC, the resistance to flow was so severe that the loading of lysis, RT, and PCR reagents was abnormal. For this reason, the collagen IFC was for the most part excluded from the data analysis. cDNA yield from each condition was assessed by Picogreen. For collagen, the average cDNA yield for single live cells following 24 hours of culture on Polaris was an average of 0.48 ng per cell, whereas for all other ECM conditions the yields ranged from approximately 4 to 9 ng per cell. The approximately 10-fold lower yield for collagen corroborates the observed poor loading of lysis/RT/PCR reagents on the collagen IFC.

### 3.3. Laminin increases motility in single-cell and bulk culture

The motility of single cells within the Polaris IFC capture sites was assessed by analyzing images taken by the Polaris system at hourly intervals during the on-IFC culture (Figure 10). The images were analyzed in ImageJ by tracing the paths of single cells for the full image sequence. Cells that exhibited zero movement during culture and stained DAPI positive after culture were omitted because it could not be determined with certainty whether

those cells were immobile due to true heterogeneity of cellular response or due instead to poor viability.

The raw numbers for motility in sample 3, which was run 3 months prior to samples 2 and 1, are greater overall, averaging 1853, 878, and 919 microns respectively for laminin-cultured cells. This may reflect differences between lots of pooled cord blood. Alternatively, despite efforts to recreate the cell handling protocols for sample 3, it is possible that variations in cell handling (thawing, culture, sorting, staining, and washing) may have arisen.

In parallel with microfluidic experiments, GMPs were also cultured in bulk to monitor morphology and provide a positive control in RT-PCR. Cells were cultured for 24h in bulk (4000 cells/well) in a 96-well round-bottom plate treated with collagen, laminin, fibronectin, vitronectin, or untreated PDMS. While the cells cultured on collagen, vitronectin, and untreated wells remained relatively close-packed, cells cultured on fibronectin were slightly more dispersed. Cells cultured on laminin displayed a markedly more dispersed behavior (**Figure 11**). A second set of wells with media + MCSF were also prepared in the same way, and had the same outcome. This was consistent for all three pooled cord blood samples and correlates well with the phenotype observed in single-cell cultures.

### 3.4.Differentially expressed genes in single cells outline motility-related signaling pathways

Single-cell cDNA libraries were quantified by Picogreen and then prepared for sequencing. Metrics for the subsequent sequencing runs are summarized in **Table 3.**

After mapping to RefSeq and removal of outliers using the Singular Analysis Toolset for R, differential gene expression analysis was performed indicating clear ECM-dependent changes between experimental conditions. Since Sample 3 was used in testing all five ECM conditions, we focused on those results first.

ANOVA analyses for single live cells on different ECMs with sample 3 identified a number of significantly differentially expressed genes (**Table 4**, **Supplementary Table 7**). The greatest number of differentially expressed genes with p-value <0.05 was identified for laminin vs PDMS: 78 genes. Beyond these ANOVA-identified genes, there are a great many more which demonstrate differential expression simply by fold-changes in expression levels between ECM conditions. PCA (principal component analysis) and tSNE (t-distributed stochastic neighbor embedding) plots of single cells demonstrate clustering by ECM, especially for laminin (**Figure 12)**. Both PCA and tSNE are statistical methods for dimensionality reduction in complex data sets that can be used to clearly identify variables, such as the expression of a given gene, that distinguish one data set from another. Both of these analysis methods yield clustering by ECM. This suggests that the gene expression data for cells of a given ECM condition are more similar to other cells of that ECM than to cells cultured on the other ECMs.

Due to the extreme differences observed in cell motility and bulk culture density for laminin in particular, further analysis on differential gene expression was focused on laminin. It has been established that laminins, and in particular laminin-521, promotes the motility of CD34+CD38- cells (31, 32). Knowing that integrins are significant in cell adhesion and migration, the gene expression data was combed for any integrins whose expression was

much higher or lower in laminin than in other ECMs. It was found that a number of genes relating to integrin signaling are preferentially expressed with laminin, including ITGAL and ITGB2, which comprise the adhesion protein LFA-1, and ITGA5 and ITGB1, which comprise the adhesion molecule VLA-5. As indicated in **Figure 13,** it appears that the laminin-cultured cells express between 2- and 12-fold higher levels of LFA-1 and VLA-5.

Inspection of expression levels for genes known in the literature to be associated with adhesion and motility revealed that a number of these genes are upregulated in the laminin cells, including RCC2, ILK, FLNA, ABLIM1, IQGAP1, IQGAP2, RAC1, and TLN1 (**Figure 13B**) (1, 33-35).

Samples 1 and 2 were analyzed to determine the reproducibility of the findings from sample 3. The gene expression analysis from samples 1 and 2 broadly align with sample 3. PCA and hierarchical clustering (**Figure 15, Figure 14**) reveal several subgroups within the laminin-cultured cells. The samples in the group termed "Ln2" are entirely from sample 1, whereas group "Ln" appears to predominantly consist of cells from sample 2. This clustering is therefore likely to be representative of heterogeneity between cord blood samples. Motility for these subgroups is represented in **Figure 16,** wherein the “Ln” and “Ln2” subgroups are approximately 6-fold and 2-fold higher than untreated PDMS, respectively. P-values for Ln vs PDMS, Ln vs Ln2, and Ln2 vs PDMS are $1.91 \times 10^{-5}$, $8.39 \times 10^{-5}$, and 0.236 respectively.

Genes whose expression appear to be zero when cultured on PDMS cannot be verified as technical dropouts or genuinely zero expressers, and have therefore been included in a separate table and labeled in the figures provided here (**Supplementary Table 11**). Due to

apparent zero expressers, much of the data is represented as differences in TPM expression values rather than fold-changes in expression.

ANOVA revealed gene sets that are differentially expressed between cells cultured on laminin vs on untreated PDMS, with the 338 differentially expressed genes found for PDMS vs subgroup "Ln." (

**Table 5**). These lists and their corresponding p values are included in **Supplementary Table 8** and **Supplementary Table 10**. The gene expression patterns for motility-related genes in samples 1 and 2 agreed with those described for sample 3 in **Figure 13** (see **Supplementary Table 9**). For the same gene set as in **Figure 13** (ITGAL, ITGB2, ITGA5, ITGB1, RCC2, ILK, FLNA, ABLIM1, IQGAP1, IQGAP2, RAC1, and TLN1) expression values in transcripts per million (TPM) were once again 2- to 20-fold higher in cells cultured on laminin than cells cultured on untreated PDMS for genes whose expression was non-zero for PDMS. For genes in that set whose expression was zero for PDMS-cultured cells, mean expression was several hundred TPM for laminin-cultured cells. This core set of genes appears to be consistently expressed more highly in GMPs cultured on laminin than in cells cultured on untreated PDMS.

Many genes coding for members of the Arp2/3 complex were overexpressed in laminin-cultured cells as compared to PDMS-cultured cells (Figure 17). The Arp2/3 complex is a central node in motility pathways - activated by Rac and CDC42 and responsible for WASP/WAVE protein activation, Arp2/3 is crucial to lamellopodial activity (19). Notably,

ARPC3 was approximately 4-fold upregulated in PDMS samples as compared to Ln samples in stark contrast with most other Arp members.

A number of additional interesting genes are many-fold overexpressed in laminin vs PDMS (**Figure 18**, **Supplementary Table 9**). Unless otherwise noted, these genes are overexpressed in laminin-cultured cells in all three samples. Small Rho GTPase RhoA is expressed at a mean of 523 and 276 TPM in Ln and Ln2 subgroups, respectively, as compared to zero expression in the untreated PDMS groups. ACTB, which codes for the beta-actin whose polymerization drives forward extension of lamellopodia, was overexpressed in samples 1 and 2, but not sample 3 (19). Also overexpressed are cofilin, integrins alpha 5 and beta 1, TUBB6, TUBB, TUBA1A, TUBA1B, which are all involved in tubulin and actin folding. DIAPH1, which codes for mDia1, as well as ROCK1 were more highly expressed in laminin than PDMS, but ROCK1P1, a pseudogene of ROCK1, was much more highly expressed for PDMS. PPP1R12A, coding for the catalytic subunit of myosin light chain phosphatase (MLCP) was more highly expressed for laminin, but PPP1R12B, coding for the myosin-binding subunit, was more highly expressed for PDMS. CDC42, which is a primary driver of motility, and several myelin action-associated genes including MYL12B and MYL6 are overexpressed (19). RPSA is a non-integrin family molecule colloquially called "The Laminin Receptor" that was overexpressed in laminin-cultured samples. CD34 is also dramatically overexpressed, suggesting that differentiation may perhaps also be impacted by laminin vs PDMS culture.

### 3.5. Differential gene expression results from MCSF dosing of single cells on Polaris

Differentially expressed genes between cells dosed with MCSF during 24-hour culture on Polaris vs untreated cells on Polaris were assessed in order to determine whether MCSF induced early expression of markers of differentiation towards a macrophage fate. A total of 11 genes were significantly differentially expressed (ANOVA p value > 0.05) consistently when assessing all ECM conditions for samples 1, 2, and 3, including FLNA which is involved in filopodial action. None of these genes were determined to be identifiably related to differentiation based on literature search. See **Supplementary Table 12** for the complete list.

# 4. Discussion

## 4.1. Choice of extracellular matrix and 4.5um bead loading can cause resistance to flow

Collagen is hard to work with in the context of microfluidics and can easily cause clogs (36). Unfortunately the collagen used for the proof of concept experiments was different from that used for the cell based experiments. The latter had to be reconstituted in lab whereas the former was provided from the manufacturer in solution. It is likely that the collagen used for cell-based experiments was not free of particulates at the start of the experiment. It is possible that by using a better-prepared collagen solution and reassessing the clogging limits on the 10um/4.5umbead mix, collagen could yet be successfully applied on Polaris.

In hindsight, it would have been preferable to repeat the proof-of-concept experiments using the 10/4.5um bead mixture to re-titrate the ECM concentrations for the new, smaller pore size. The exact mechanism by which the 4.5um beads create these issues is not yet known. The strongest theory at present is that the 4.5um beads tend to enter the small gaps at the right/top end of each capture chamber, which can reduce reagent flow including the loading of the entire bead solution, contributing to underloading.

In fibronectin-, vitronectin-, and collagen- coated capture chambers, accumulation of materials on the far side of the bead pack was visible (**Figure 19**). These aggregations, while previously not observed, were likely composed of the ECM itself caused by poor flow rates through the capture site due to decreased sieve pore size caused by the inclusion of the 4.5um beads. These aggregates likely reduced the facility of reagent flow-through in subsequent steps following prime.

The Polaris workflow has already been validated from start to finish with the 10um bead formulation using 25ng/uL fibronectin as the ECM. Thus it stands to reason that with optimization, it should not be unreasonable to see good results using 50ng/uL with the 10um beads, or to see good results with a lower concentration with the 10um/4.5um bead mix. Follow-up experiments are required to further optimize fibronectin. Because vitronectin and fibronectin performed similarly in this set of experiments, it is expected that vitronectin can also be fully adapted to the Polaris workflow with further tuning of the concentration used for a given bead mix formulation.

The laminin chip used for sample 3 had no issues either relating to the bead packs or resistance to flow. It was therefore determined that 50ng/uL laminin is safe and effective for use on Polaris chips. These conditions were repeated for samples 1 and 2 with only mild resistance to flow. The untreated PDMS chip for sample 1 had much higher resistance to flow than any of the laminin chips, supporting the theory that for compatible ECMs, variability in how tightly the 4.5um beads are wedged into the capture site features is an important factor in resistance to flow (see **Table 2**).

### 4.2.Culture of granulocyte-macrophage progenitors on Polaris successfully yields cDNA for sequencing

Despite the issues described above, GMP cells were successfully captured and cultured, and generated cDNA that produced high-quality sequencing data demonstrating that this cell type is compatible with Polaris. Despite the difficulty in detecting low-expressed genes in

single cells such as transcription factors, meaningful gene sets have been identified in the data differentiating each of the ECM conditions (11).

The most highly expressed genes across the dataset largely represent ribosomal proteins, DNA replication, transcription, translation and similar macromolecular processes. This indicates that the cells are indeed successfully cultured on Polaris and are responding to the cytokines in the media, which include Flt3L, SCF, IL-3, and IL-6, with normal cellular processes (see **Supplementary Table 6**). However, the relatively low viability of these cells on Polaris as compared to model cell lines such as K562s and BJ fibroblasts in internal R&D experiments suggests that singulated culture may be overall more stressful for these cells. Other primary cells cultured for 24 hours on Polaris have similar viability and retention rates to the ones observed for GMPs here. For comparison, BJ fibroblasts on average have a successful viability rate of 92% as determined by Zombie Yellow staining. Despite potential differences between stringency of Zombie Yellow as compared to DAPI in identifying dead or dying cells, this suggests that these primary cells are less amenable to singulated culture than robust cell lines. Until orthogonal single-cell culture technologies are developed, the question of whether this degree of viability is normal or could be negatively impacted by the Polaris instrument itself remains unanswered.

### 4.3. Sequencing metrics and data normalization

Although the sequencing data for sample 3 was robust, the library was under-tagmented for the samples 1 and 2, resulting in low mapping to RefSeq and Genome (See **Table 3**). However, given the large total number of reads, it was determined that the raw number of

mapping reads was still sufficient for the data analysis required and as such the expense of re-running the library prep and sequencing was not necessary. Unfortunately, the severe differences in library quality between S3 vs S1 and S2 make it very challenging to compare the two data sets accurately. Normalization is a challenge in single-cell mRNA Seq data even when technical replicates are apparently very similar. This is due to inherent cell-to-cell heterogeneity and the high proportion of zero read counts that occur due to sheer lack of expression of some genes or dropouts due to technical limitations. There does not exist at present a standardized normalization method using housekeeping genes for this particular combination of challenging conditions – that is, single-cell mRNAseq with granulocyte-macrophage progenitors where the extracellular matrix and motility are major variables. Many traditional housekeeping genes such as ACTB and CD34 are directly impacted by these experimental conditions and therefore cannot be relied upon in this case (37, 38). It is beyond the scope of this thesis to develop or adapt an adequate set of housekeeping genes for this cell type that can be used reliably for normalization, although this could hypothetically be done in future studies. Accordingly, the two data sets were not analyzed together. It is still valuable to compare the analyses that result from these two separate data sets, though it is prudent to compare them more in qualitative terms than quantitative ones. Note that the data was normalized to TPM (transcripts per million) without issue, and this should be sufficient to directly compare data within each sequencing run.

An additional consideration taken into account in this analysis was that there was a partial IFC malfunction during PCR on the IFC containing sample 2 cells on unmodified PDMS. Consequently, a lower volume of PCR reagents than normal was loaded for all cells on this IFC. This resulted in poorer overall amplification, and it cannot be ruled out whether

601 flawed or nonlinear amplification may have occurred as a result. Thus a greater proportion of
602 samples from this IFC were rejected by outlier analysis than any other IFC. In analyzing
603 fold-changes in expression, care was taken not to include samples that had zero expression
604 from this IFC, as this would indicate dropouts due to non-linear amplification (38). Wherever
605 zero expressers are used in the data analysis, they are called out so that the analysis
606 performed with these cells must be done cautiously.

607

608 **4.4. Gene expression analysis suggests small Rho GTPases drive motility**

609 Several members of the complex network of interactions that drive cell motility have
610 been observed to be overexpressed in granulocyte-macrophage progenitors in single-cell
611 culture on laminin in this work. Myosin II is responsible for the lengthwise movement of
612 antiparallel actin filaments that results in contraction via hydrolysis-driven actin filament
613 formation (19, 22). Its essential light chains come in three isoforms: myosin IIA, IIB, or IIC.
614 Each complete myosin II molecule is comprised of two of these essential light chains, two
615 regulatory light chains, and two heavy chains. Thr18 and Ser19 of myosin II's regulatory
616 light chains are reversibly phosphorylated by Rho GTPases to regulate its activity. When
617 myosin II activity is interrupted, extension rates at the leading edge increase and adhesion
618 sizes decrease, indicating that myosin II is required for stable adhesion structure formation
619 and maintenance, but not the initial protrusion (19, 22). While the processes of contraction
620 and extension may therefore appear to be in opposition, they are in fact complementary; a
621 moving cell oscillates between extension and contraction (23, 24). Thus, concurrent

622 expression of proteins involved in both processes is indicative that both processes may be
623 happening more than in a less motile cell.

624 Just as extension, adhesion, and contraction all influence one another, ECM ligation,
625 integrin clustering, and actin polymerization are all connected by a high degree of interplay
626 (26). CDC42 and Rac activate WASP and WAVE (WASP-family verprolin homologue,
627 a.k.a. SCAR) proteins, which in turn activate the seven-subunit Arp2/3 complex which
628 induces actin nucleation and subsequent polymerization, thereby causing extension (19, 24,
629 39). CDC42 and Rac also activate PAK Ser/Thr kinases which activate myosin II through
630 phosphorylation of its regulatory light chains, driving contraction. PAKs also inhibit cofilin –
631 cofilin promotes disassembly of actin, so through this interaction PAK contributes to
632 sustained actin polymerization. Similarly, RhoA can influence both extension and
633 contraction. RhoA at the front of the cell combines with mDia1 present at the tips of
634 filopodia to promote actin polymerization and extension, whereas RhoA at the rear of the cell
635 activates ROCK (Rho-associated protein kinase) proteins, which inhibit myosin
636 phosphatases, allowing myosin II to remain phosphorylated and active (23, 40). This network
637 of interactions is represented in **Figure 20**, with genes overexpressed in laminin culture in
638 this body of data shown in blue.

639 Our data clearly showed differential expression of several integrins, suggesting
640 increased production of VLA-5 (ITGA5/ITGB1) and LFA-1(ITGAL/ITGB2) in laminin-
641 cultured cells. LFA-1 may be expressed preferentially in CD34+ cells naturally circulating in
642 peripheral blood than in bone marrow, suggesting a possible connection between LFA-1
643 expression and increased movement rather than adhering stably to the extracellular

environment (26, 41-43). Interestingly, VLA-5 is canonically a fibronectin-binding protein (1). However it has also been demonstrated to induce migration via a pathway that involves filamin-A (FLNA), RCC2, IQ-motif proteins including IQGAP1, and Rac1 (33-35). Rac1 is also known to be regulated by integrin-linked kinase (ILK), via IQGAP1 and parvins, to impact motility and lamellopodium formation (44). We observed each of these genes to be overexpressed in laminin culture relative to PDMS only. Another differentially expressed gene was ABLIM1, which has been demonstrated to interact with F-actin in a manner that correlates with increased motility of hematopoietic cells (45-47). PMP22 was also differentially expressed; PMP22 is a binding partner in the integrin/laminin complex and is involved in mediating the interaction of HSCs with the extracellular environment (48). Together these results present additional potential explanations for the marked difference in motility observed with single cells cultured on laminin vs other ECMs.

One alternative factor which could be driving cell motility is the cytokine interleukin 6 (IL-6), which was present in the culture media. IL-6 has been demonstrated to increase the expression of PMP22 (49). SCF and FTL3, also present in the media, are also known to induce mobilization. A possible explanation could be that these cytokines induce higher motility in the presence of laminin, although why laminin-cultured cells would preferentially respond to IL-6, SCF, and FLT3 is yet unclear (49). Another possibility is that laminin's effect on motility is independent of these molecules. Future studies that test whether the exclusion of these factors impacts motility would be enlightening.

One of the questions raised by this data is why the cells move extensively if there is nominally no significant gradient of ECM in the culture sites on IFC. We know from the

initial work of this study that the deposition of ECMs on Polaris, while not dramatically uneven, is prone to slight non-uniformity (see **Figure 5B**). However, the movement of the cells was not observed to trend in any particular direction or stop once the cells reached a single area of the culture chambers. An explanation for this apparent discrepancy is that in integrin-mediated motility, initiation of lamellopodium formation is at first random in direction, and positive feedback loops then favor a single direction, often based on extracellular cues (24). This characteristic is called directional persistence, and it depends on the degree of lamellopodial persistence, which is in turn determined by the degree of balance between actin nucleation and polymerization according to the mechanisms described previously in this section. Rac activation induced by signals from activated integrins causes recruitment and localization of more integrins, and so on, creating a self-sustaining response in one region that becomes the leading edge (19, 26, 50). As a result, even a modest gradient may trigger a dramatic haptotactic response.

### 4.5. Gene expression analysis is inconclusive regarding differentiation

Because this set of experiments included only 24 hours of single-cell culture on each ECM with and without MCSF treatment, the changes observed are necessarily for early markers of any processes that may have been initiated by the experimental conditions. Canonically, it takes 7 to 14 days of culture for differentiation to occur in vitro (51). It may be that with a culture timeline extended to several days with a greater number of replicates, more signs of altered differentiation would become apparent. There does not appear to be an abundance of data on differential gene expression in early

MCSF-treated GMPs in the literature, so although this work is novel, it is also challenging to establish new patterns and observations with certainty.

It is notable that CD34 is consistently and extremely differentially expressed between laminin and PDMS in all three GMP samples regardless of MCSF treatment. CD34 is a canonical marker for GMPs, and is one of the primary markers selected for in the FACS scheme used to purify the GMP population used in these experiments. Expression of CD34 was approximately 13-fold higher expressed for laminin-cultured cells than for cells cultured on untreated PDMS, suggesting that laminin is maintaining the cells in their initial state of differentiation, whereas PDMS may be driving either differentiation towards a more mature state or dedifferentiation to an earlier progenitor. It would be useful to observe the initial state of CD34 expression using a rapid workflow such as Fluidigm's C1™ system in order to have a more robust basis of comparison. Regarding MCSF treatment, one gene of interest that was more highly expressed in MCSF-treated cells was FLN1, or Fibulin 1 (52). Fibulin 1 binds ECM proteins including laminin and fibrinogen. How this may relate to MCSF dosing is unclear. Again, further studies using a greater number of cells and longer timeframes may yield more conclusive results.

# 5. Conclusion and Future Directions

The Polaris system for single-cell culture and cDNA generation is compatible with laminin at 50 ng/uL, broadening the range of experimental conditions that researchers may use with the system. Granulocyte-macrophage progenitors purified by FACS are amenable to 24 hour culture on Polaris, and the resulting cDNA libraries yield illuminating differential expression data via transcriptome sequencing. Analysis of this data determined that extracellular matrices can indeed cause differential gene expression. Laminin induced distinct phenotypic and genotypic changes in the GMPs. Phenotypically, cells cultured on laminin-coated PDMS displayed a two- to six-fold increase in motility relative to untreated PDMS. This increase in motility was paralleled by altered expression of a number of genes, including integrin-mediated signaling pathways. Integrin signaling emerged as a particularly compelling story due to concurrent overexpression of small Rho GTPase RhoA as well as 2- and 4-fold increases in Rac1 and CDC42 respectively. Further strengthening the integrin signaling idea, 4 to 6-fold increases in cytoskeletal and motility-associated genes ILK, FLNA, ABLIM1, and IQGAP2, and genes that code for the ARP2/3 complex were observed. It is clear from this data that a response is being elicited in these cells relating to motility. These responses were confirmed to be recapitulated in multiple different pooled cord blood samples, though the degree of the response is variable. Future work would evaluate more lots of pooled cord blood to further understand the degree of uniformity or heterogeneity between samples.

Naturally, this leads to the question of whether these changes impact differentiation in these GMPs. The 13-fold difference in CD34 expression in cells cultured on laminin relative

to untreated PDMS suggests that there may indeed be some impact, but within the short time frame of these experiments the impact on final cell fate is unclear. Because differentiation typically requires approximately ten days of culture, future directions for this work include longer-range experiments to determine the precise fate of the cells. Altogether, these experiments tell us that ECM choice in single-cell culture can be critical to conscientious experimental design, where cell fate and motility are involved.

# 6. Tables

**Table 1.** Summary of results for proof-of-concept ECM deposition on the Polaris system.

| ECM | Imaging/Staining Method | Recommendation |
|---|---|---|
| Fibronectin | Fluorescently-labeled fibronectin (FAM) | Maximum 50 ng/uL |
| Laminin | Fluorescently-labeled laminin (FAM) | Maximum 50 ng/uL |
| Vitronectin | Unlabeled vitronectin, SimplyBlue SafeStain secondary stain (semi-quantitative) (CY5) | Maximum 50 ng/uL |
| Collagen | Native fluorescence of unlabeled collagen (semi-quantitative) (CY5) | Maximum 50 ng/uL |
| Matrigel | Unlabeled matrigel (CY5) | Not recommended for use on Polaris |

**Table 2.** Polaris IFC run outcomes including bead packs, cell selection accuracy, cell retention during culture, and viability by DAPI following culture. Ideal Polaris IFC runs using model cell types such as K562s have approximately 46-48 single cells selected, 40 or more cells retained during culture, and at least 35 live cells following culture.

| | Bead Pack Qualities | | | |
|---|---|---|---|---|
| | Sample | Under-packing | Resistance to Flow | Bead Pack Movement After Prime |
| **PDMS** | 3 | Mild | None | Moderate |
| **Laminin** | 3 | None | None | None |
| **Fibronectin** | 3 | Moderate | Moderate | None |
| **Vitronectin** | 3 | Mild | Moderate | None |
| **Collagen** | 3 | Severe | Severe | None |
| **PDMS** | 2 | Mild | Mild | None |
| **Laminin** | 2 | None | Mild/Moderate | None |
| **PDMS** | 1 | Moderate | Severe | None |
| **Laminin** | 1 | None | Mild/Moderate | None |

| | | Cell Selection | | Post-Culture | |
|---|---|---|---|---|---|
| | Sample | # Sites With Multiple Cells | # Single Cells | # Cells Retained | # Single Live Cells (DAPI negative or dim) |
| **PDMS** | 3 | 2 | 37 | 26 | 17 |
| **Laminin** | 3 | 1 | 43 | 31 | 18 |
| **Fibronectin** | 3 | 9 | 21 | 20 | 2 |
| **Vitronectin** | 3 | 10 | 20 | 15 | 5 |
| **Collagen** | 3 | 4 | 3 | 6 | 5 |
| **PDMS** | 2 | 1 | 46 | 44 | 37 |
| **Laminin** | 2 | 5 | 72 | 71 | 29 |
| **PDMS** | 1 | 3 | 15 | 15 | 1 |
| **Laminin** | 1 | 9 | 66 | 60 | 35 |

**Table 3.** Sequencing metrics for samples 1, 2, and 3. Samples 1 and 2 were prepped and sequenced in a single library, whereas sample 3 was prepped and run separately.

| | **Data Set** | **Sample 3** | **Samples 1 & 2** |
|---|---|---|---|
| | Number of samples sequenced | 168 | 288 |
| | Percent > Q30 | 89% | 86% |
| Metrics For Single Live Cells | Total Reads | 6,651,308 | 4,692,947 |
| | Read hits aligned to RefSeq | 1,877,912 | 331,776 |
| | Percent Mapping to RefSeq | 23.1% | 5.3% |
| | Read hits aligned to Genome | 4,253,755 | 1,309,962 |
| | Percent Mapping to Genome | 54.7% | 25.4% |

**Table 4.** Number of genes identified by ANOVA with $p < 0.05$ for sample 3 Using Singular Analysis Toolset for R to analyze RefSeq-mapped data expressed in transcripts per million (TPM), ANOVA identified differentially expressed between sample groups.

| | Laminin | Fibronectin | Vitronectin |
|---|---|---|---|
| Fibronectin | 9 | - | - |
| Vitronectin | 48 | 2 | - |
| PDMS | 78 | 1 | 4 |

**Table 5.** Number of genes identified by ANOVA with $p < 0.05$ for samples 1 and 2. Using Singular Analysis Toolset for R to analyze RefSeq-mapped data expressed in transcripts per million (TPM), ANOVA identified differentially expressed between sample groups defined by PCA.

| | **Ln** | **Ln2** | **PDMS** |
|---|---|---|---|
| **Ln** | - | - | - |
| **Ln2** | 316 | - | - |
| **PDMS** | 338 | 360 | - |

# 7. Figures

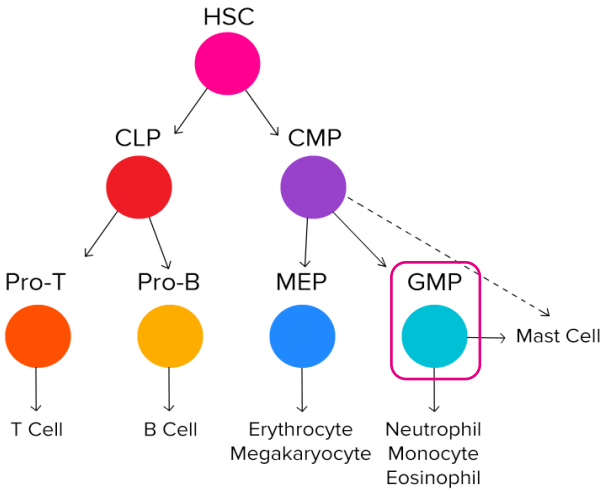


**Figure 1.** Schematic of hematopoiesis. Hematopoiesis may be represented in a simplified manner as illustrated here. Hematopoietic stem cells (HSCs) may self-renew or differentiate into either the lymphoid or myeloid lineages, giving rise to common lymphoid or myeloid progenitors (CLP or CMP), respectively. Granylocyte-macrophage progenitors (GMP) arise from CMPs (1).

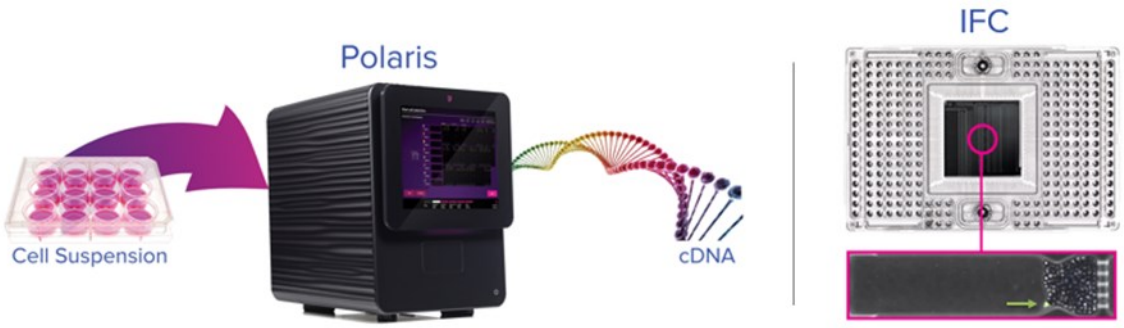


**Figure 2.** The Polaris™ system

The Polaris benchtop instrument and general workflow (left) and an integrated fluidic circuit (IFC) "chip" (right) with a single cell in a microfluidic capture site (green arrow). The IFC is approximately the size of an index card.

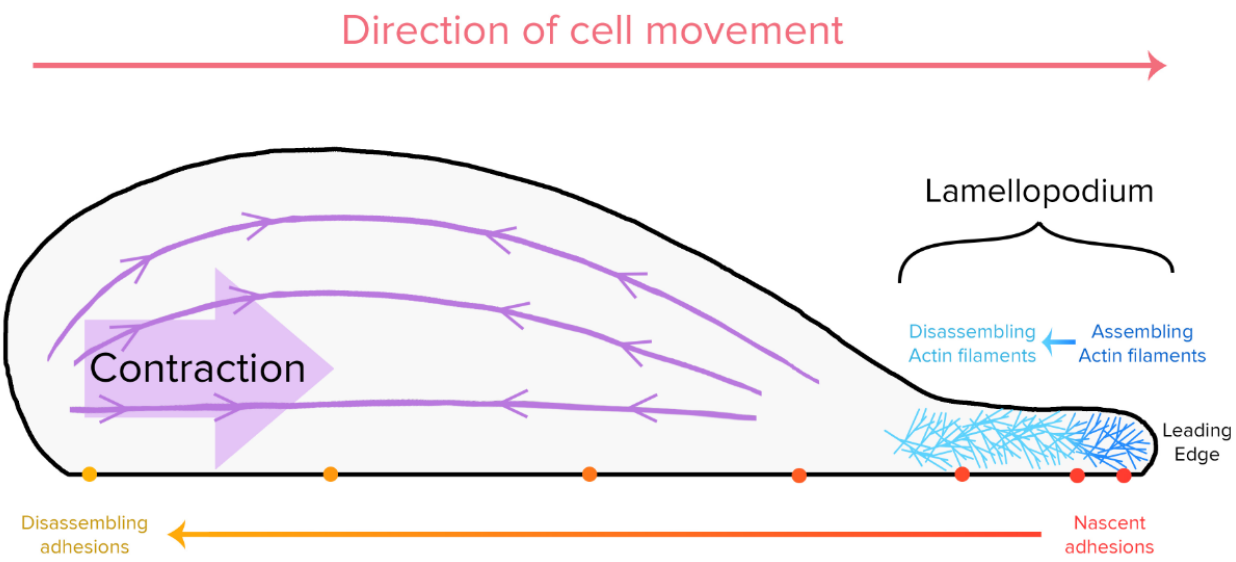


768

769 **Figure 3.** Mechanism of cell motility

770 At the leading edge of the cell, assembling actin filaments extend lamellopodia forward,
771 prevented from slipping backwards by nascent adhesions on the bottom surface of the
772 cell. At the rear end of the lamellopodium, actin filaments disassemble, maintaining the
773 total actin present at the front of the cell. As the cell shifts forwards, adhesions age and
774 ultimately disassemble. Actomyosin contraction along the length of the cell pulls the rear,
775 unanchored end of the cell forward. Adapted from Ananthakrisnan & Erlicher (2002)
776 (21).

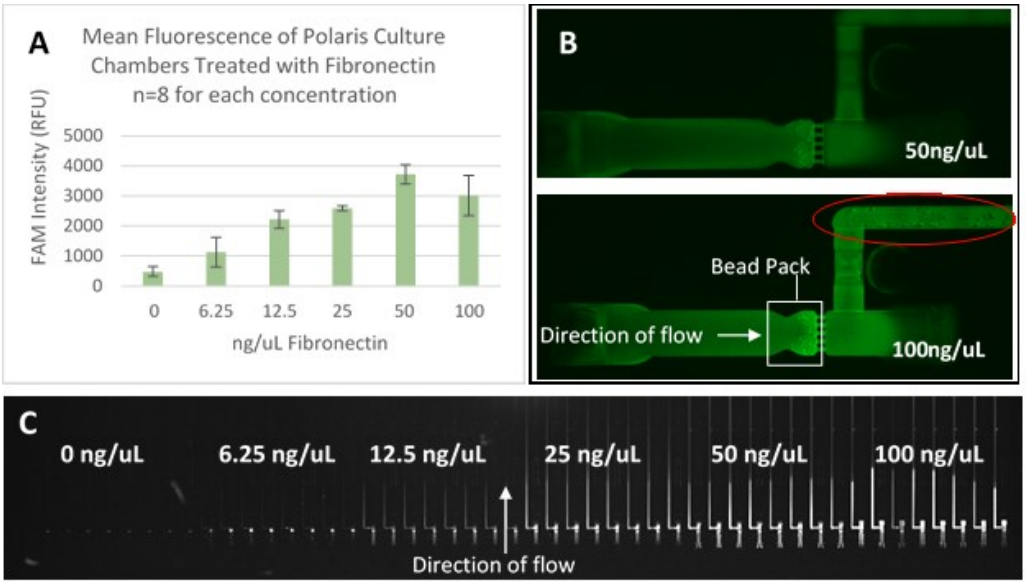


**Figure 4.** Fibronectin deposition on Polaris

A) Fluorescence intensity following deposition of fluorescent fibronectin on Polaris IFC. Images were taken in FAM at 20X magnification. Fluorescence was measured using ImageJ for each capture site and averaged for each concentration. Error bars represent standard deviation. B) Images of Polaris IFC chambers coated with fibronectin, with particulates visible at 100 ng/uL (red circle). C) FAM image taken using Polaris' native imaging system demonstrating increasing fluorescence intensity with increasing concentration of fibronectin.

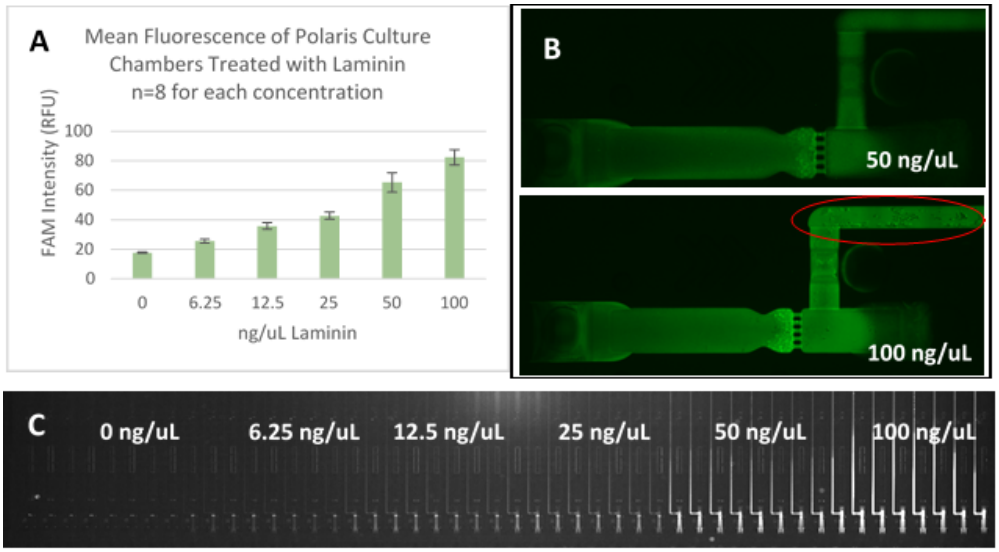


**Figure 5.** Laminin deposition on Polaris

A) Fluorescence intensity following deposition of fluorescent laminin on Polaris IFC. Images were taken in FAM at 20X magnification. Fluorescence was measured using ImageJ for each capture site and averaged for each concentration. Error bars represent standard deviation. B) Images of Polaris IFC chambers coated with laminin, with particulates visible at 100ng/uL (red circle). C) FAM image taken using Polaris' native imaging system demonstrating increasing fluorescence intensity with increasing concentration of laminin.

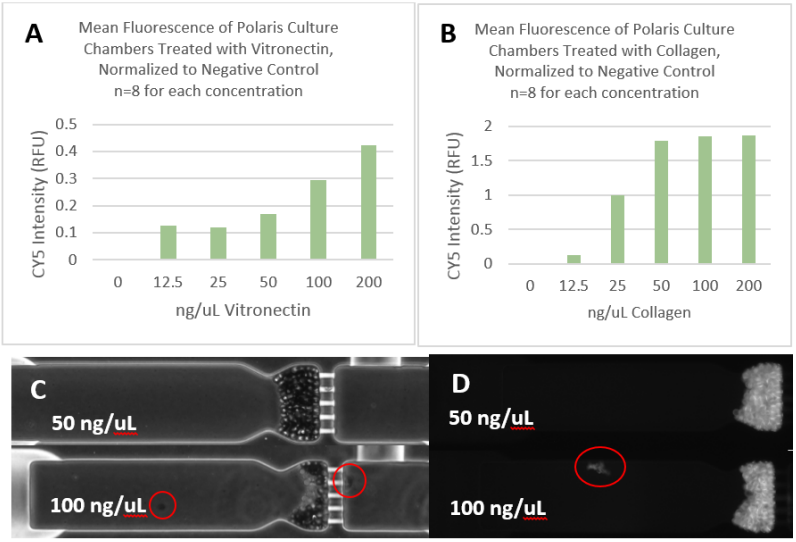


**Figure 6.** Vitronectin and collagen deposition on Polaris.

796

797 Fluorescence intensity in CY5 following deposition of vitronectin (A) and collagen (B)
798 on Polaris IFC. Images were taken in CY5 at 20X magnification. Fluorescence was
799 measured using ImageJ for each capture site and averaged for each concentration.
800 Particulates are visible and circled in red starting at 100ng/uL both in vitronectin in phase
801 contrast (C) and collagen in CY5 (D).

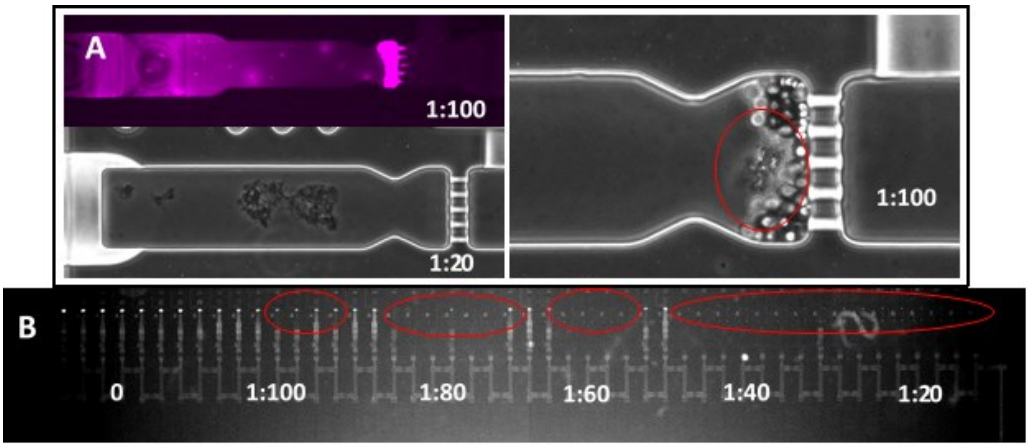


**Figure 7.** Matrigel deposition on Polaris

A) 20X magnification images in CY5 and phase contrast on a Polaris IFC of attempted deposition of matrigel. Particulates and clogs are evident. Dilution of matrigel (1:100, 1:20, etc.) are labeled in each image. B) CY5 image taken using the Polaris system's native imaging system showing impaired or failed bead loading (red circles) in all cases except the negative control, indicating severe clogs.

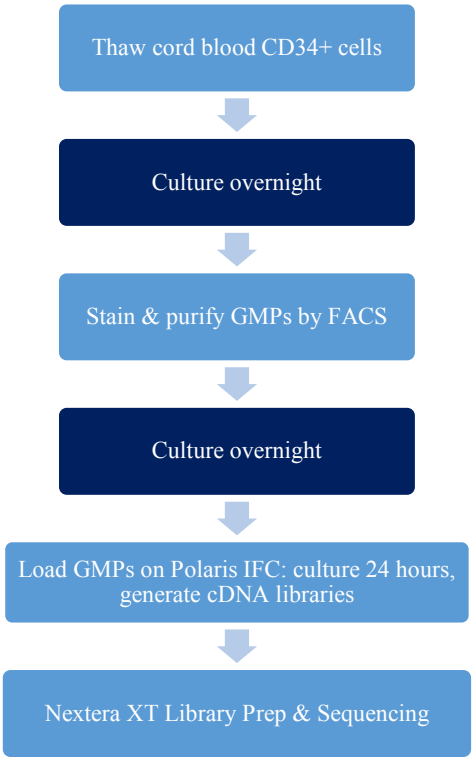


807

808 **Figure 8.** Workflow for GMP experiments on Polaris

809 Frozen cord blood CD34+ cells were cultured overnight after thawing, and again after

810 purification of the GMP population by FACS. The cells were then loaded onto the Polaris

811 IFC and cultured for 24-hours. The output of the Polaris system is single-cell cDNA

812 libraries, which were then prepped for sequencing.

813

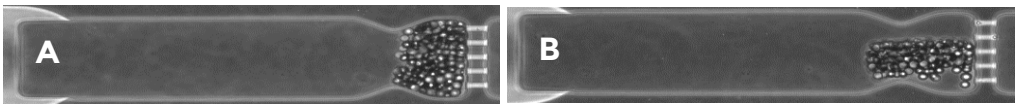


814

815 **Figure 9.** Bead packs on Polaris

816 A) Normal bead pack and B) underloaded and dislodged bead pack. Phase contrast

817 images taken at 20X magnification.

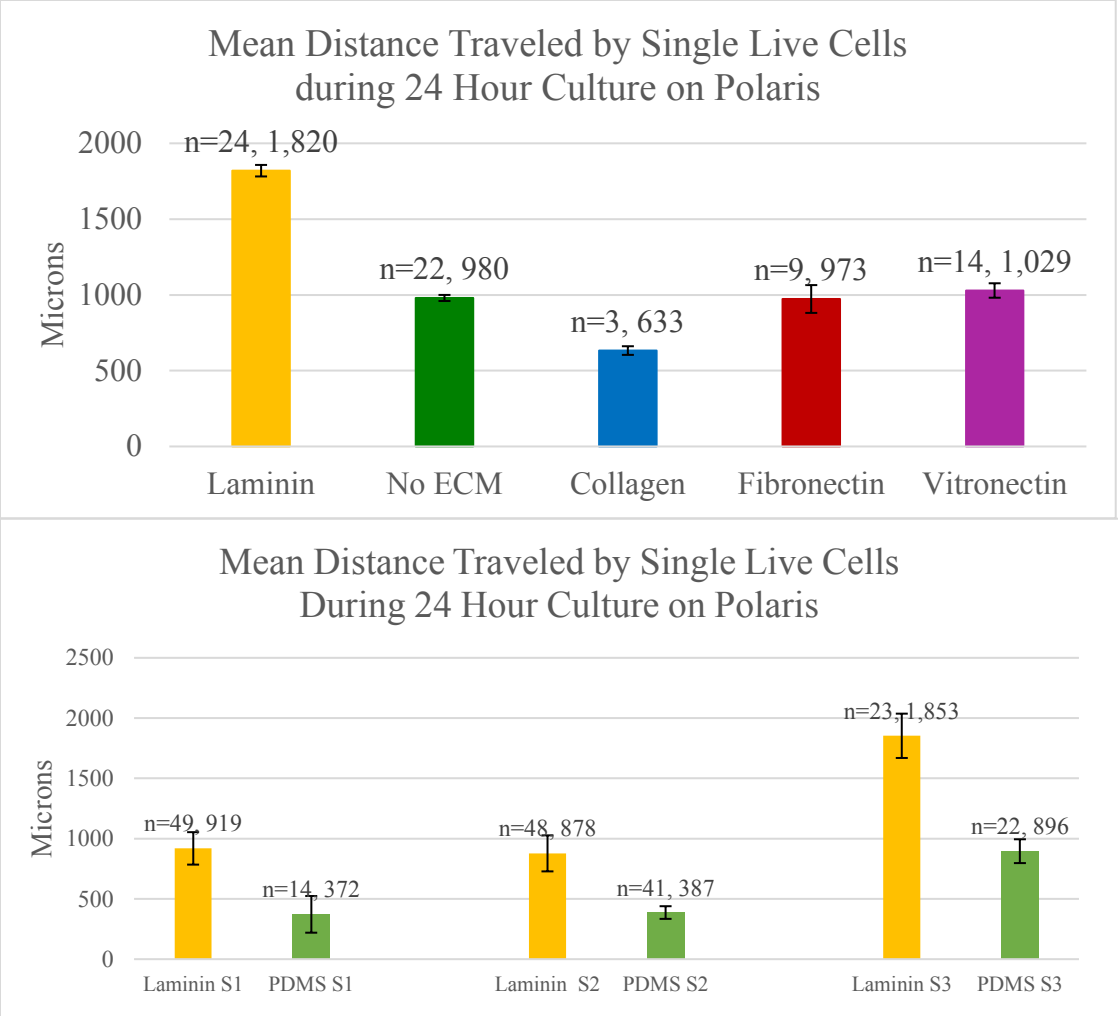


**Figure 10.** Motility during single-cell culture on Polaris.

Motility of single cells cultured on the Polaris system for 24 hours, excluding DAPI-positive cells. A) Sample 3, and B) for all three samples. Images were taken automatically every hour by the Polaris system in VIC and FAM channels. ImageJ was used to measure the distance moved by single, live cells between each image and summed for each cell and converted from pixels to microns using the known dimensions of the chip features. Error bars represent standard error of the mean (SEM).

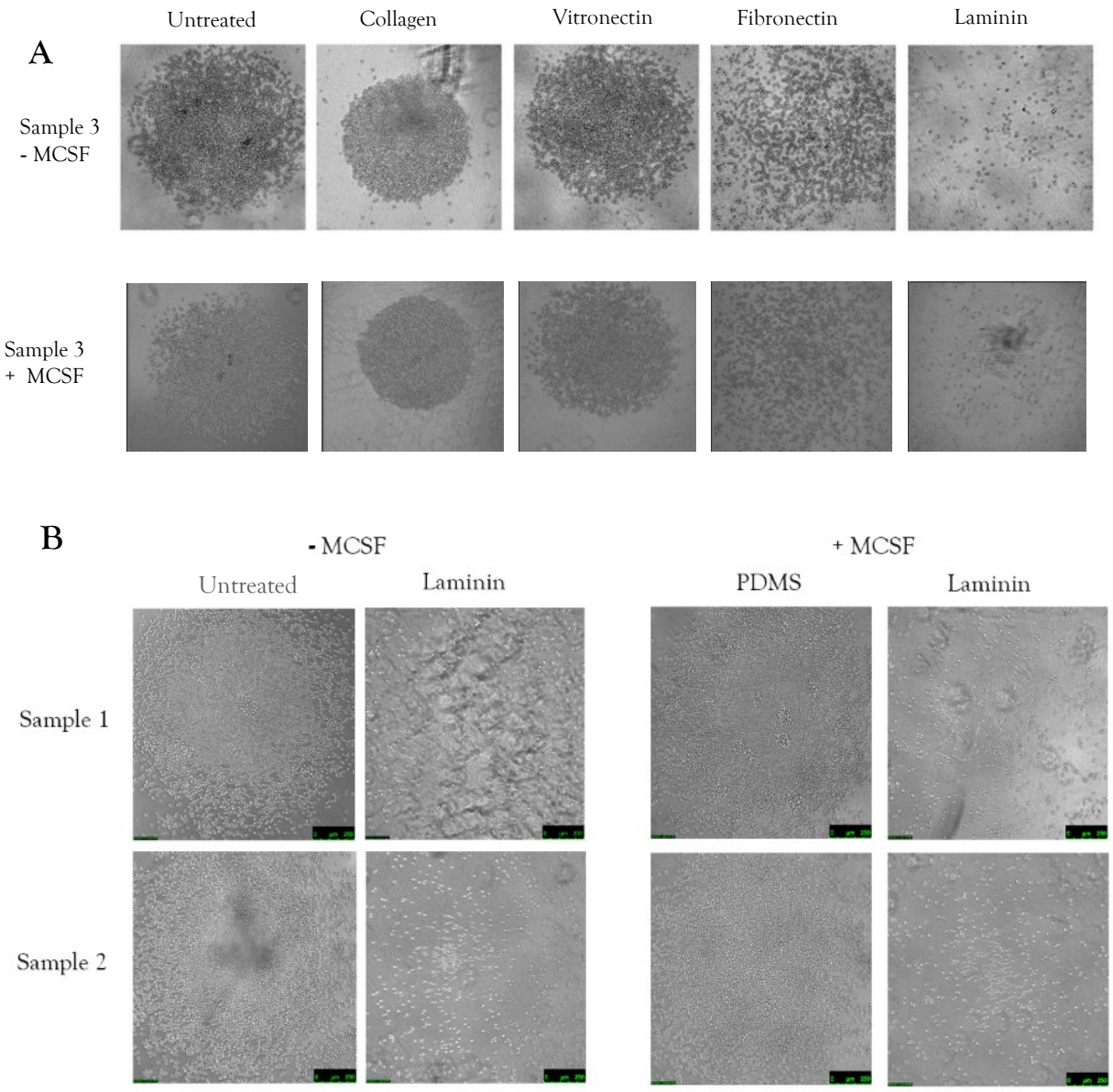


**Figure 11.** Bulk-cultured GMPs on different ECMs have different densities

824 4000 GMP cells were sorted into round-bottom 96-well plates and cultured for 24 hours.
825 Phase contrast images were then taken at 10X magnification. The differential appearance
826 in cell motility phenotypes between laminin and untreated wells appears to be maintained
827 both with and without MCSF. This is true for both sample 3 (A) and samples 1 and 2 (B).

828

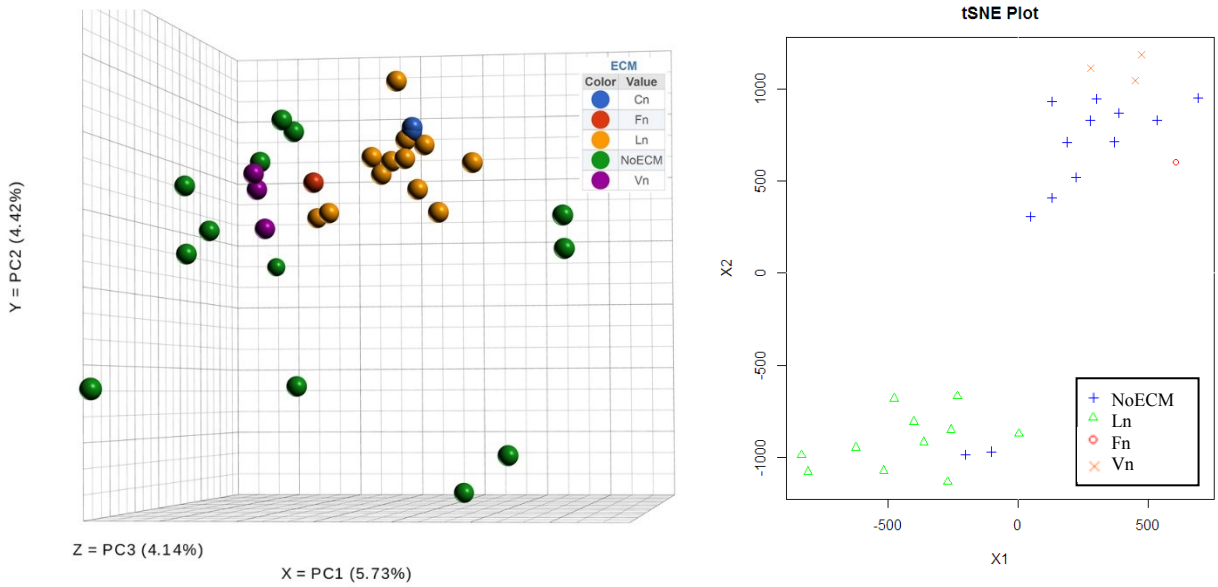


**Figure 12.** PCA and tSNE for Sample 3 GMPs cultured on Polaris

829 Using Singular Analysis Toolset for R to analyze RefSeq-mapped data expressed in
830 transcripts per million (TPM), principal component analysis and tSNE for single live
831 cells in sample 3 demonstrated clustering of laminin-cultured cells relative to cells
832 cultured on untreated PDMS. NoECM: untreated PDMS; Ln: laminin; Fn: fibronectin;
833 Vn: vitronectin; Cn: collagen.

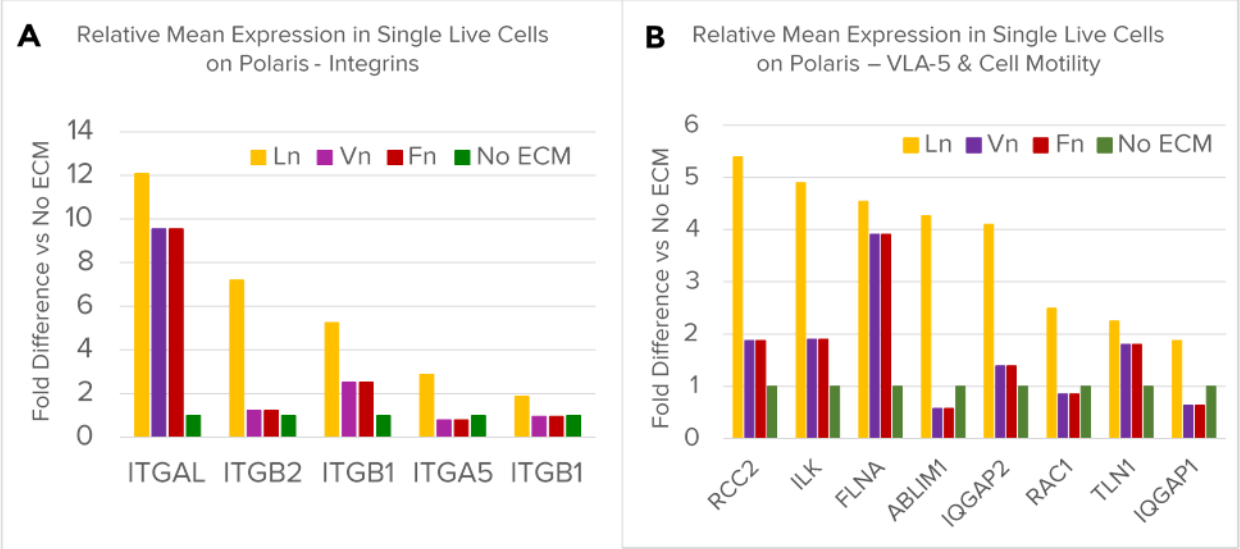


834

835 **Figure 13.** Fold-difference in expression of genes comprising LFA-1 and VLA-5 in

836 sample 3 GMPs.

837 A) Expression of several integrins that compose LFA-1 and VLA-5 are higher in laminin-

838 cultured cells for Sample 3, represented here in fold-difference of transcripts per million

839 (TPM) relative to cells cultured on "No ECM" (untreated PDMS). B) As in A), fold

840 difference in expression of several genes associated with VLA-5 function are more highly

841 expressed in laminin-cultured cells.

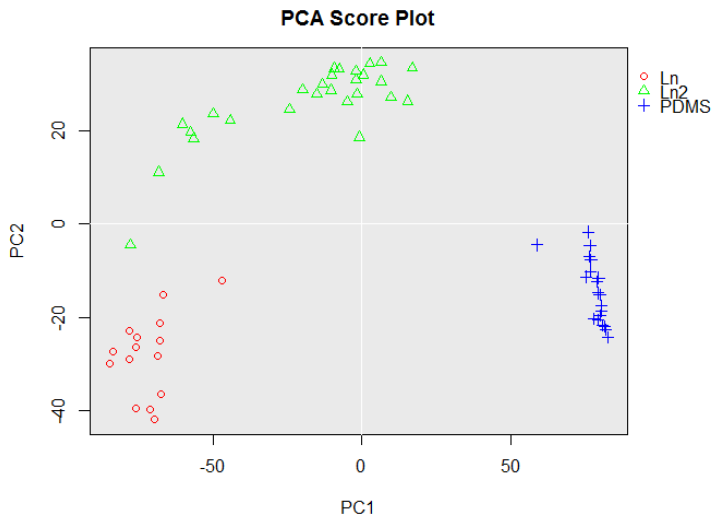


842

843 **Figure 14.** Principal component analysis for GMP samples 1 and 2

844 Using Singular Analysis Toolset for R to analyze RefSeq-mapped data expressed in
845 transcripts per million (TPM), Sample 1 and 2 single, live GMPs were segregated into
846 groups based on clustering by PCA. Here, those groups are represented as “Ln,” “Ln2,”
847 and “PDMS.” These group assignments were used in subsequent analyses.

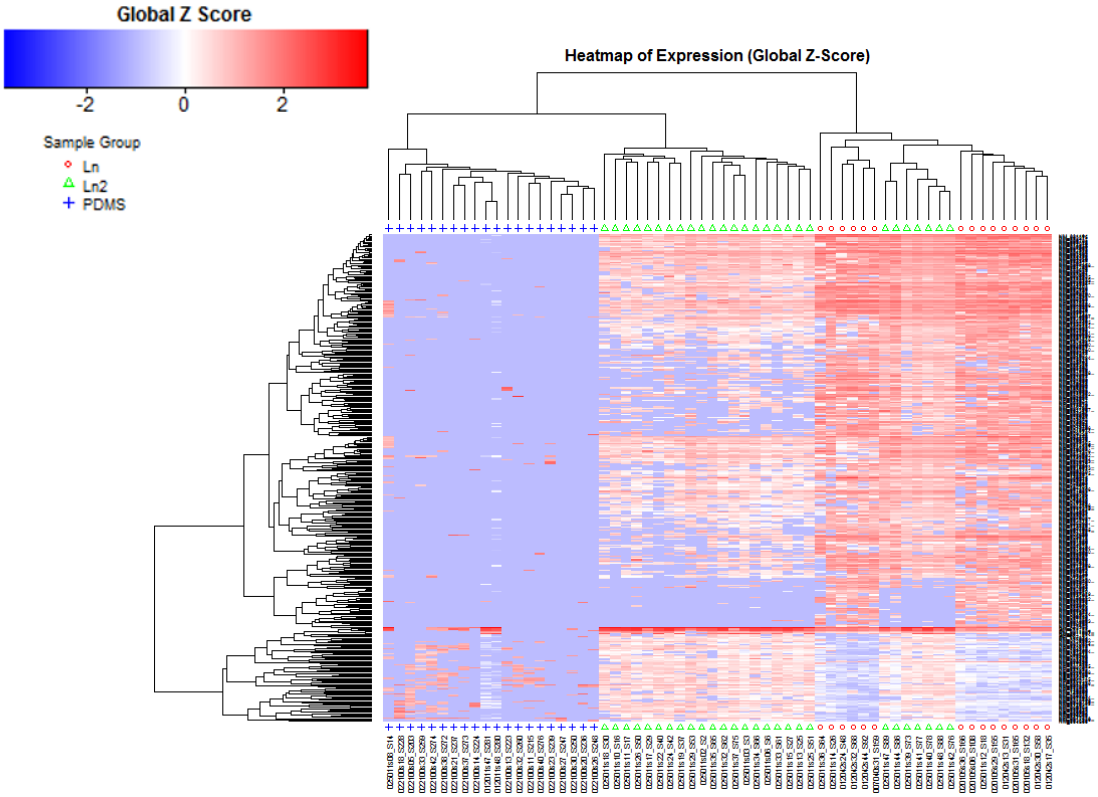


**Figure 15.** Hierarchical clustering of cells cultured on laminin and PDMS for Samples 1 and 2

Using Singular Analysis Toolset for R to analyze RefSeq-mapped data expressed in transcripts per million (TPM), laminin-cultured were segregated into groups based on PCA analysis (see previous Figure). Hierarchical clustering using these groups demonstrated clear delineations between GMPs cultured on PDMS and laminin, as well as between laminin subgroups ("Ln" and "Ln2").

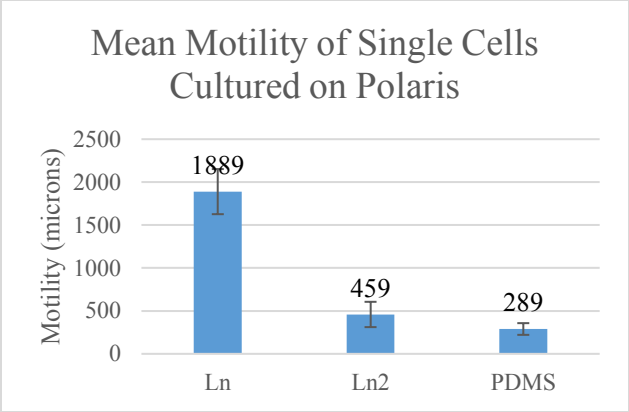


856

857 **Figure 16.** Motility of GMP subgroups during single-cell culture

858 The motility of single live cells in samples 1 and 2 grouped by PCA clustering as in

859 **Figure 14** were analyzed as described in **Figure 10**. Error bars represent standard error of

860 the mean.

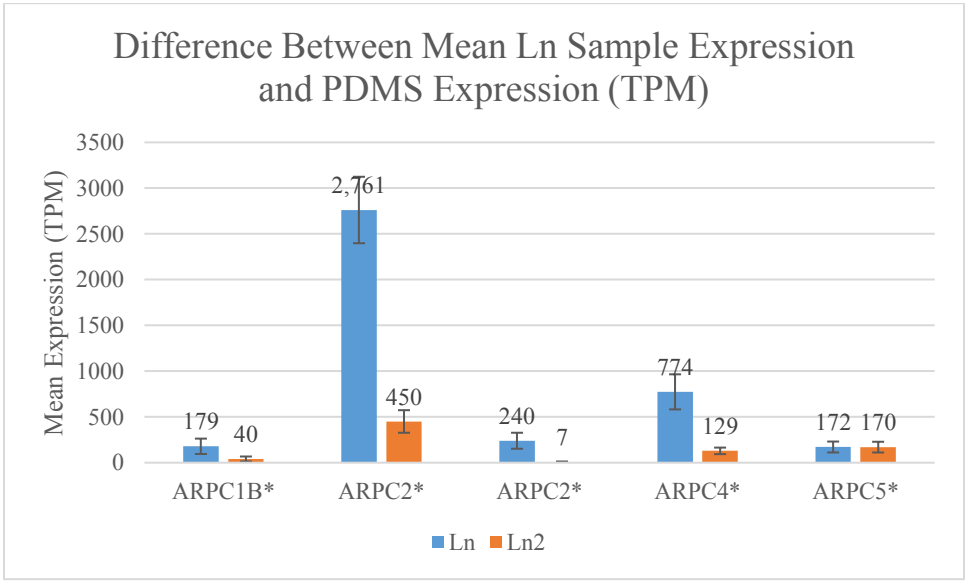


861

862 **Figure 17.** Overexpression of genes coding for the Arp2/3 complex

863 The difference in gene expression measured in transcripts per million (TPM) between

864 laminin-cultured cells in subgroups “Ln” and “Ln2” and untreated PDMS demonstrates

865 that genes coding for components of the Arp2/3 complex are more highly expressed in

laminin-cultured cells than for cells cultured on PDMS. Genes with zero expression in PDMS-cultured cells are marked with an asterisk. Error bars represent standard error of the mean.

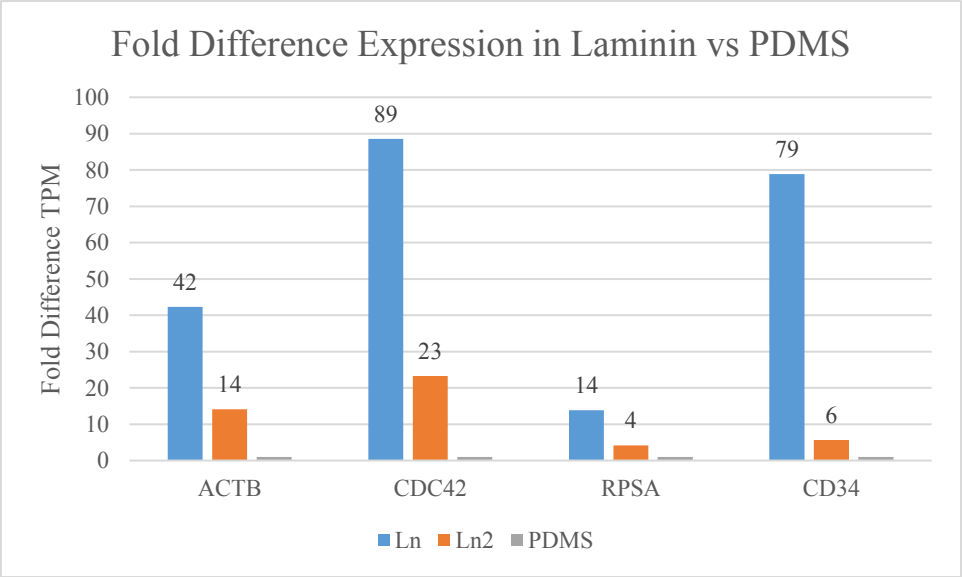


**Figure 18.** Differential expression of genes of interest in GMP Samples 1 and 2. The fold-difference in gene expression measured in transcripts per million (TPM) between laminin-cultured cells in subgroups "Ln" and "Ln2" and untreated PDMS demonstrates that the genes indicated here are more highly expressed in laminin-cultured cells than for cells cultured on PDMS.

877

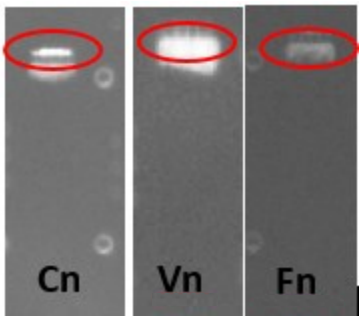


**Figure 19.** ECM accumulation on downstream side of bead packs.

878 ECM materials aggregated (circled in red) on the far side of bead packs in collagen,
879 vitronectin, and fibronectin-coated capture sites, from automated Polaris images taken
880 after completion of the prime step using 50 ng/uL of the indicated ECM protein.

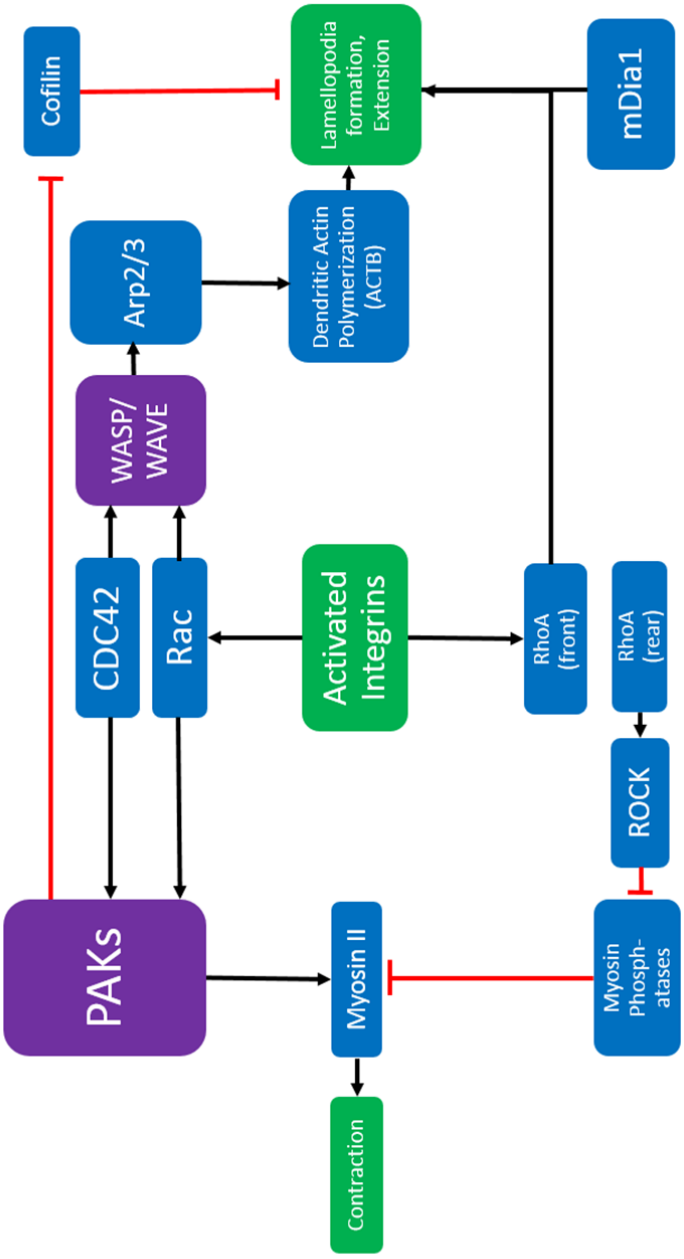


881

882 **Figure 20.** Small Rho GTPases CDC42, Rac, and RhoA drive motility in a complex
883 network of interactions. Blue: genes observed to be overexpressed in single-cell culture
884 on laminin relative to untreated PDMS. Purple: genes unconfirmed in this work. Green:
885 events putatively occurring inside or outside the cell.

# 8. Appendices

**Supplementary Table 1.** FACS sorting scheme for pooled cord blood cells. Lineage markers used were CD7, CD10, CD19, CD11b, CD235a, and CD14.

| **Emission Wavelength (nm)** | 450/50 | 525/50 | 600/60 | 720/60 |
|---|---|---|---|---|
| **FL #** | **FL1** | **FL2** | **FL3** | **FL5** |
| **Final choice** | **Bv421** | **AF488** | **PE** | **PerCp Cy5.5** |
| **Marker** | **CD34** | **Lin-** | **FLT3 (aka CD135)** | **CD45RA** |

**Supplementary Table 2.** FACS sorting antibodies for pooled cord blood cells.

| Vendor | Catalogue # | Product Name | Sort +/- |
|---|---|---|---|
| Biolegend | 343103 | FITC anti-Human CD7 | - |
| Biolegend | 312207 | FITC anti-Human CD10 | - |
| Biolegend | 302219 | FITC anti-Human CD19 | - |
| Biolegend | 343609 | BV421 anti-Human CD34 | + |
| Biolegend | 301317 | AF488 anti-Human CD11b | - |
| Biolegend | 303514 | AF647 anti-Human CD38 | - |
| Biolegend | 306609 | FITC anti-Human CD235a | - |
| Biolegend | 303623 | AF488 anti-Human CD41 | - |
| Biolegend | 304121 | PerCp Cy5.5 anti-Human CD45RA | + |
| BD Biosciences | 561706 | AF488 anti-Human CD14 | - |
| BD Biosciences | 558996 | PE anti-Human CD135 | + |

**Supplementary Table 3.** FACS sorting plate layout for bulk culture and single-cell plate culture for Sample 3.

| Plate | 1 | 2 | 3 | 4 | 5 | 6 | 7 | 8 | 9 | 10 | 11 | 12 |
|---|---|---|---|---|---|---|---|---|---|---|---|---|
| **A** | C | C | L | L | V | V | F | F | NO ECM | NO ECM | BULK C | **BULK C + MCSF** |
| **B** | C | C | L | L | V | V | F | F | NO ECM | NO ECM | BULK L | **BULK L + MCSF** |
| **C** | C | C | L | L | V | V | F | F | NO ECM | NO ECM | BULK V | **BULK V + MCSF** |
| **D** | C | C | L | L | V | V | F | F | NO ECM | NO ECM | BULK F | **BULK F + MCSF** |
| **E** | C | C | L | L | V | V | F | F | NO ECM | NO ECM | BULK NO ECM | **BULK NO ECM + MCSF** |
| **F** | C | C | L | L | V | V | F | F | NO ECM | NO ECM | Empty | Empty |
| **G** | C | C | L | L | V | V | F | F | NO ECM | NO ECM | Empty | Empty |
| **H** | C | C | L | L | V | V | F | F | NO ECM | NO ECM | Empty | Empty |
| | **SINGLE CELLS** | | | | | | | | | | **BULK** | |
| | **100uL/well StemSpan + CC100** | | | | | | | | | | | |

**Supplementary Table 4.** FACS sorting plate layout for bulk culture and single-cell plate culture for Samples 1 and 2.

| Plate | 1 | 2 | |
|---|---|---|---|
| **A** | BULK L | **BULK L + MCSF** | Sample 1 |
| **B** | BULK L | **BULK L + MCSF** | |
| **C** | BULK NO ECM | **BULK NO ECM + MCSF** | |
| **D** | BULK NO ECM | **BULK NO ECM + MCSF** | |
| **E** | BULK L | **BULK L + MCSF** | Sample 2 |
| **F** | empty | empty | |
| **G** | BULK NO ECM | **BULK NO ECM + MCSF** | |
| **H** | empty | empty | |
| **100uL StemSpan SFEM II/CC100 per well** | | | |

**Supplementary Table 5.** FACS sorting calibration plate to assess accuracy of single-cell sorting. CD34 cells were FACS sorted into a round-bottom 96-well plate according to the target cell numbers and layout indicated in the table below. After allowing the cells to settle by gravity for four hours, the cells were imaged under a 10X phase microscope and the number of cells in each well was counted.

| | 1 | 2 | 3 | 4 | 5 | 6 | 7 | 8 | 9 | 10 | 11 | 12 | # of Cells Sorted | | |
|---|---|---|---|---|---|---|---|---|---|---|---|---|---|---|---|
| | | | | | | | | | | | | | Intended | Observed | |
| | | | | | | | | | | | | | | Average | Stdev |
| **A** | 1 | 1 | 1? | 0 | 1 | 1 | 1 | 1 | 1 | 1 | 1 | 1 | **1** | 0.91 | 0.30 |
| **B** | 9 | 7 | 9 | 8 | 10 | 10 | 9 | 10 | 9 | 10 | 10 | 8 | **10** | 9.08 | 1.00 |
| **C** | 17 | 20 | 17 | 16 | 16 | 18 | 17 | 18 | 18 | 17 | 20 | 17 | **20** | 17.58 | 1.31 |
| **D** | 36 | 39 | 38 | 36 | 35 | 39 | 36 | 35 | 39 | 39 | 38 | 36 | **40** | 37.17 | 1.64 |

**Supplementary Table 6.** Top 500 expressed genes for sample 3 and their gene ontology annotations via PANTHER GO.

| Gene Ontology Annotations (PANTHER GO): Biological Process | No. of Genes | Percentage of Total Function Hits |
|---|---|---|
| **Metabolic process (GO:0008152)** | 247 | 32.4% |
| **Cellular process (GO:0009987)** | 240 | 31.5% |
| **Cellular component organization or biogenesis (GO:0071840)** | 105 | 13.8% |
| **Localization (GO:0051179)** | 41 | 5.4% |
| **Response to stimulus (GO:0050896)** | 39 | 5.1% |
| **Biological regulation (GO:0065007)** | 33 | 4.3% |
| **Developmental process (GO:0032502)** | 19 | 2.5% |
| **Immune system process (GO:0002376)** | 17 | 2.2% |
| **Multicellular organismal process (GO:0032501)** | 14 | 1.8% |
| **Reproduction (GO:0000003)** | 3 | 0.4% |
| **Biological adhesion (GO:0022610)** | 2 | 0.3% |
| **Locomotion (GO:0040011)** | 2 | 0.3% |

**Supplementary Table 7.** Differentially expressed genes in single live cells on different ECMs with ANOVA p value < 0.05 for sample 3: 112 genes total.

| Number of genes with p < 0.05 | 130 | 9 | 1 | 2 | 78 | 48 | 4 |
|---|---|---|---|---|---|---|---|
| GeneID | Anova.p Value | Ln vs Fn | PDMS vs Fn | Vn vs Fn | PDMS vs Ln | Vn vs Ln | Vn vs PDMS |
| FIBP | 0.000 | 1.000 | 0.368 | 0.038 | 0.002 | 0.000 | 0.083 |
| DDX39B | 0.000 | 0.020 | 0.653 | 0.515 | 0.000 | 0.065 | 0.924 |
| HLA-DRB5 | 0.000 | 0.072 | 0.825 | 1.000 | 0.001 | 0.002 | 0.511 |
| NGDN | 0.000 | 0.032 | 0.410 | 1.000 | 0.008 | 0.001 | 0.107 |
| HCST | 0.000 | 0.687 | 0.777 | 0.999 | 0.000 | 0.202 | 0.583 |
| CPSF3L | 0.000 | 0.232 | 0.997 | 0.969 | 0.001 | 0.003 | 0.664 |
| SNX3 | 0.001 | 0.042 | 0.281 | 1.000 | 0.073 | 0.001 | 0.040 |
| NCOA4 | 0.001 | 0.394 | 1.000 | 0.976 | 0.002 | 0.015 | 0.892 |
| ZNHIT3 | 0.001 | 1.000 | 0.536 | 0.146 | 0.011 | 0.003 | 0.296 |
| MTX1 | 0.002 | 0.125 | 0.743 | 1.000 | 0.014 | 0.005 | 0.336 |
| METTL1 | 0.002 | 0.046 | 0.579 | 0.748 | 0.004 | 0.055 | 0.993 |
| NUP107 | 0.002 | 0.051 | 0.599 | 0.777 | 0.004 | 0.054 | 0.989 |
| MRPS23 | 0.002 | 0.108 | 0.709 | 0.999 | 0.013 | 0.008 | 0.464 |
| WBP5 | 0.002 | 0.940 | 0.880 | 0.337 | 0.014 | 0.003 | 0.255 |
| HLA-DRB1 | 0.002 | 0.122 | 0.842 | 0.978 | 0.004 | 0.029 | 0.924 |
| NUBP1 | 0.002 | 0.013 | 0.002 | 0.004 | 0.234 | 0.501 | 0.997 |
| STX8 | 0.002 | 1.000 | 0.556 | 0.129 | 0.023 | 0.004 | 0.224 |
| NDUFA11 | 0.002 | 0.552 | 0.994 | 0.950 | 0.003 | 0.024 | 0.945 |
| MIEN1 | 0.002 | 1.000 | 0.631 | 0.129 | 0.037 | 0.003 | 0.158 |
| GIMAP7 | 0.002 | 1.000 | 0.731 | 0.123 | 0.067 | 0.002 | 0.087 |
| IFT74 | 0.003 | 0.109 | 0.564 | 0.999 | 0.053 | 0.007 | 0.247 |
| ERGIC3 | 0.003 | 0.226 | 0.923 | 1.000 | 0.011 | 0.017 | 0.694 |
| CDC45 | 0.004 | 0.987 | 0.980 | 0.196 | 0.288 | 0.002 | 0.024 |
| SSNA1 | 0.004 | 0.138 | 0.889 | 0.612 | 0.003 | 0.498 | 0.716 |
| CHCHD5 | 0.004 | 0.077 | 0.462 | 0.969 | 0.051 | 0.015 | 0.400 |
| PPID | 0.004 | 0.985 | 0.465 | 0.123 | 0.040 | 0.008 | 0.309 |
| STRAP | 0.004 | 0.825 | 0.948 | 0.748 | 0.008 | 0.020 | 0.785 |
| TUBB4B | 0.005 | 0.343 | 0.999 | 0.917 | 0.003 | 0.400 | 0.780 |
| PGAP2 | 0.005 | 0.997 | 0.326 | 0.581 | 0.003 | 0.230 | 0.957 |
| BRCC3 | 0.005 | 0.025 | 0.250 | 0.457 | 0.030 | 0.130 | 0.977 |
| PPA2 | 0.005 | 0.708 | 0.118 | 0.091 | 0.020 | 0.062 | 0.907 |
| IL2RG | 0.005 | 0.059 | 0.564 | 0.510 | 0.009 | 0.293 | 0.977 |
| IMP4 | 0.005 | 0.997 | 0.363 | 0.404 | 0.006 | 0.090 | 0.998 |
| COPS7A | 0.005 | 0.065 | 0.226 | 0.967 | 0.338 | 0.012 | 0.112 |
| CDKAL1 | 0.005 | 0.964 | 0.220 | 0.640 | 0.004 | 0.543 | 0.705 |
| STRN4 | 0.006 | 0.793 | 0.113 | 0.394 | 0.007 | 0.531 | 0.793 |
| DNAJC15 | 0.006 | 0.172 | 0.656 | 1.000 | 0.087 | 0.010 | 0.238 |
| ERLIN1 | 0.006 | 0.042 | 0.426 | 0.261 | 0.014 | 0.622 | 0.812 |
| PCID2 | 0.007 | 0.054 | 0.278 | 0.885 | 0.136 | 0.025 | 0.358 |
| UBA3 | 0.007 | 0.989 | 0.624 | 0.118 | 0.129 | 0.007 | 0.141 |
| SNURF | 0.007 | 0.179 | 0.762 | 0.999 | 0.038 | 0.021 | 0.542 |
| ZNF317 | 0.007 | 0.514 | 0.918 | 0.818 | 0.240 | 0.005 | 0.068 |
| R3HCC1 | 0.007 | 0.152 | 0.862 | 0.704 | 0.007 | 0.393 | 0.904 |
| DAP | 0.007 | 0.031 | 0.257 | 0.503 | 0.047 | 0.135 | 0.954 |
| TBL2 | 0.008 | 0.010 | 0.076 | 0.061 | 0.106 | 0.832 | 0.908 |
| MYCBP | 0.009 | 0.988 | 0.436 | 0.232 | 0.027 | 0.033 | 0.723 |
| MND1 | 0.009 | 1.000 | 0.496 | 0.431 | 0.012 | 0.072 | 0.966 |

| | | | | | | | |
|---|---|---|---|---|---|---|---|
| POLD3 | 0.009 | 1.000 | 0.460 | 0.653 | 0.007 | 0.227 | 0.990 |
| IGLL1 | 0.009 | 0.595 | 1.000 | 0.622 | 0.010 | 0.999 | 0.114 |
| DHCR7 | 0.010 | 0.945 | 0.522 | 0.099 | 0.184 | 0.011 | 0.171 |
| ACAA2 | 0.010 | 0.145 | 0.785 | 0.820 | 0.015 | 0.205 | 1.000 |
| PLIN3 | 0.010 | 0.975 | 0.338 | 0.996 | 0.016 | 0.992 | 0.109 |
| TGFBRAP1 | 0.011 | 1.000 | 0.486 | 0.904 | 0.007 | 0.643 | 0.684 |
| DDX50 | 0.011 | 0.135 | 0.565 | 0.981 | 0.095 | 0.033 | 0.490 |
| PRC1 | 0.012 | 0.216 | 0.858 | 0.256 | 0.024 | 0.999 | 0.169 |
| GDE1 | 0.013 | 0.169 | 0.781 | 0.924 | 0.025 | 0.118 | 0.976 |
| TOMM34 | 0.014 | 0.179 | 0.467 | 1.000 | 0.379 | 0.019 | 0.152 |
| DDX23 | 0.014 | 1.000 | 0.601 | 0.499 | 0.021 | 0.084 | 0.950 |
| DBF4B | 0.016 | 0.488 | 0.998 | 1.000 | 0.017 | 0.124 | 0.993 |
| RBM4B | 0.017 | 0.611 | 0.913 | 0.102 | 0.456 | 0.128 | 0.015 |
| TIMM17A | 0.017 | 0.233 | 0.386 | 1.000 | 0.816 | 0.022 | 0.068 |
| COX7C | 0.018 | 1.000 | 0.554 | 0.500 | 0.024 | 0.117 | 0.977 |
| AGBL5 | 0.018 | 0.469 | 0.077 | 0.495 | 0.056 | 0.998 | 0.421 |
| PCCB | 0.019 | 0.977 | 0.981 | 0.447 | 0.217 | 0.014 | 0.180 |
| HPS1 | 0.021 | 0.595 | 1.000 | 0.992 | 0.031 | 0.082 | 0.911 |
| CDC20 | 0.021 | 0.701 | 0.997 | 1.000 | 0.015 | 0.256 | 0.998 |
| TPRKB | 0.021 | 0.481 | 0.931 | 0.974 | 0.156 | 0.025 | 0.329 |
| LOC401397 | 0.021 | 0.915 | 0.946 | 0.844 | 0.027 | 0.087 | 0.933 |
| SNRPN | 0.022 | 0.232 | 0.686 | 0.998 | 0.159 | 0.042 | 0.454 |
| PLSCR1 | 0.022 | 0.999 | 0.560 | 0.493 | 0.031 | 0.124 | 0.970 |
| HNRNPA0 | 0.022 | 0.117 | 0.531 | 0.831 | 0.085 | 0.139 | 0.902 |
| SRSF10 | 0.023 | 0.359 | 0.954 | 0.995 | 0.033 | 0.134 | 0.975 |
| NDUFV1 | 0.023 | 0.457 | 0.978 | 1.000 | 0.045 | 0.073 | 0.840 |
| EIF4A2 | 0.023 | 0.642 | 0.999 | 0.957 | 0.058 | 0.046 | 0.678 |
| METTL17 | 0.023 | 0.179 | 0.767 | 0.813 | 0.036 | 0.292 | 1.000 |
| FTSJ1 | 0.023 | 0.987 | 0.659 | 0.210 | 0.189 | 0.027 | 0.317 |
| LYPLA2 | 0.024 | 0.985 | 0.594 | 0.237 | 0.126 | 0.038 | 0.478 |
| PSMC4 | 0.024 | 0.995 | 0.457 | 0.955 | 0.020 | 0.951 | 0.455 |
| LCLAT1 | 0.025 | 0.962 | 0.601 | 0.171 | 0.237 | 0.029 | 0.289 |
| UBE2C | 0.026 | 0.979 | 0.445 | 0.395 | 0.043 | 0.148 | 0.971 |
| LOC388796 | 0.026 | 0.956 | 0.889 | 0.887 | 0.023 | 0.182 | 0.999 |
| RBMX | 0.027 | 0.522 | 0.992 | 0.999 | 0.043 | 0.095 | 0.903 |
| PSENEN | 0.027 | 0.246 | 0.778 | 0.985 | 0.087 | 0.091 | 0.796 |
| ANKRD39 | 0.027 | 1.000 | 0.619 | 0.717 | 0.024 | 0.264 | 1.000 |
| TMCC1 | 0.028 | 0.948 | 0.997 | 0.224 | 0.826 | 0.064 | 0.017 |
| AIFM1 | 0.028 | 0.733 | 0.188 | 0.845 | 0.064 | 0.997 | 0.256 |
| CCND3 | 0.029 | 0.817 | 0.990 | 0.963 | 0.030 | 0.137 | 0.981 |
| ANXA6 | 0.029 | 0.996 | 0.533 | 0.503 | 0.039 | 0.168 | 0.986 |
| NDC80 | 0.029 | 0.086 | 0.455 | 0.448 | 0.074 | 0.557 | 0.991 |
| CCDC124 | 0.029 | 0.925 | 0.398 | 0.238 | 0.090 | 0.094 | 0.800 |
| PPIH | 0.029 | 0.293 | 0.908 | 0.930 | 0.035 | 0.282 | 1.000 |
| BANF1 | 0.029 | 0.584 | 0.999 | 1.000 | 0.031 | 0.169 | 0.993 |
| PAFAH1B3 | 0.030 | 0.290 | 0.661 | 1.000 | 0.341 | 0.039 | 0.283 |
| ZNF613 | 0.030 | 0.564 | 0.999 | 1.000 | 0.030 | 0.180 | 0.996 |
| CCNB2 | 0.030 | 0.999 | 0.518 | 0.887 | 0.021 | 0.724 | 0.780 |
| CENPE | 0.031 | 0.582 | 1.000 | 0.836 | 0.022 | 0.939 | 0.503 |
| SYPL1 | 0.032 | 0.906 | 0.283 | 0.565 | 0.035 | 0.606 | 0.929 |
| ATP6V0D1 | 0.033 | 0.992 | 0.462 | 0.745 | 0.027 | 0.549 | 0.936 |
| BAK1 | 0.034 | 0.700 | 0.450 | 0.074 | 0.729 | 0.044 | 0.152 |
| CSTF1 | 0.035 | 0.964 | 0.459 | 0.334 | 0.075 | 0.128 | 0.899 |
| TIMP1 | 0.035 | 0.992 | 0.528 | 0.484 | 0.049 | 0.176 | 0.980 |
| HLA-DPA1 | 0.037 | 0.303 | 0.863 | 0.977 | 0.071 | 0.166 | 0.951 |
| KATNB1 | 0.037 | 0.994 | 0.520 | 0.996 | 0.041 | 1.000 | 0.274 |
| RAD1 | 0.039 | 0.941 | 0.987 | 0.715 | 0.129 | 0.047 | 0.528 |
| C9orf78 | 0.039 | 0.290 | 0.846 | 0.969 | 0.075 | 0.176 | 0.954 |

| | | | | | | | |
|---|---|---|---|---|---|---|---|
| DALRD3 | 0.039 | 0.358 | 0.084 | 0.129 | 0.186 | 0.528 | 1.000 |
| MAPRE1 | 0.039 | 0.636 | 0.855 | 0.925 | 0.734 | 0.029 | 0.103 |
| NMRAL1 | 0.041 | 0.907 | 0.439 | 0.217 | 0.167 | 0.093 | 0.677 |
| HLA-DRA | 0.041 | 0.644 | 1.000 | 0.999 | 0.046 | 0.177 | 0.983 |
| TAOK3 | 0.041 | 0.251 | 0.765 | 0.244 | 0.104 | 0.985 | 0.258 |
| TIMM8B | 0.041 | 0.298 | 0.898 | 0.821 | 0.043 | 0.544 | 0.971 |
| PAPSS1 | 0.042 | 0.703 | 0.260 | 0.980 | 0.209 | 0.723 | 0.113 |
| ETFDH | 0.043 | 1.000 | 0.711 | 0.476 | 0.092 | 0.098 | 0.805 |
| TRIM14 | 0.043 | 0.415 | 0.828 | 0.162 | 0.283 | 0.556 | 0.082 |
| COPS3 | 0.043 | 0.373 | 0.891 | 0.998 | 0.106 | 0.118 | 0.832 |
| FAS | 0.044 | 0.612 | 0.999 | 1.000 | 0.044 | 0.224 | 0.997 |
| PLP2 | 0.045 | 0.513 | 0.994 | 0.815 | 0.035 | 0.904 | 0.644 |
| POP5 | 0.045 | 0.666 | 0.985 | 0.952 | 0.207 | 0.049 | 0.442 |
| MGST3 | 0.045 | 0.230 | 0.626 | 0.974 | 0.239 | 0.105 | 0.635 |
| C6orf108 | 0.046 | 0.996 | 0.567 | 0.595 | 0.052 | 0.266 | 0.999 |
| GGCT | 0.046 | 0.709 | 0.290 | 0.133 | 0.267 | 0.125 | 0.664 |
| MYEOV2 | 0.046 | 0.516 | 0.989 | 0.998 | 0.051 | 0.240 | 0.997 |
| TIMM10 | 0.047 | 0.902 | 0.497 | 0.193 | 0.270 | 0.075 | 0.502 |
| EGFL7 | 0.048 | 1.000 | 0.600 | 0.826 | 0.036 | 0.540 | 0.962 |
| AURKB | 0.048 | 0.940 | 0.456 | 0.312 | 0.118 | 0.145 | 0.868 |
| TNFRSF10B | 0.048 | 0.566 | 0.999 | 0.907 | 0.034 | 0.800 | 0.776 |
| TIPRL | 0.048 | 0.968 | 0.588 | 0.281 | 0.193 | 0.081 | 0.602 |
| PSMB8 | 0.048 | 0.643 | 0.999 | 1.000 | 0.054 | 0.201 | 0.987 |
| TUBG1 | 0.049 | 0.384 | 0.919 | 0.990 | 0.081 | 0.190 | 0.960 |
| C6orf70 | 0.049 | 0.650 | 1.000 | 1.000 | 0.046 | 0.263 | 0.999 |
| FAM96B | 0.050 | 0.972 | 0.987 | 0.636 | 0.237 | 0.045 | 0.389 |
| MRPS15 | 0.051 | 0.572 | 0.886 | 0.975 | 0.466 | 0.044 | 0.245 |
| PMS1 | 0.053 | 1.000 | 0.912 | 0.395 | 0.370 | 0.042 | 0.284 |
| MELK | 0.055 | 1.000 | 0.675 | 0.887 | 0.040 | 0.582 | 0.952 |
| TRAPPC4 | 0.059 | 0.986 | 0.836 | 0.261 | 0.599 | 0.046 | 0.201 |
| MRFAP1L1 | 0.059 | 0.874 | 0.980 | 1.000 | 0.036 | 0.622 | 0.924 |
| PLAUR | 0.065 | 1.000 | 0.694 | 0.889 | 0.048 | 0.589 | 0.961 |

**Supplementary Table 8**. Genes identified by ANOVA distinguishing cells cultured on laminin vs PDMS and between apparent laminin subgroups in samples 1 and 2. Average values represent Log2 transformed transcripts per million (TPM).

| AccessionID | GeneID | Anova pValue | Ln2_vs_Ln pValue | PDMS_vs_Ln pValue | PDMS_vs_Ln2 pValue | Ln Average | Ln2 Average | PDMS Average |
|---|---|---|---|---|---|---|---|---|
| NM_000993 | RPL31 | 1.29E-11 | 1.08E-04 | 2.93E-12 | 6.79E-05 | 1.04E+01 | 5.36E+00 | 6.37E-01 |
| NM_002444 | MSN | 7.53E-15 | 4.08E-01 | 6.05E-12 | 1.06E-10 | 6.99E+00 | 5.84E+00 | 4.07E-01 |
| NM_018109 | MTPAP | 8.39E-14 | 3.75E-02 | 1.78E-11 | 4.14E-08 | 7.46E+00 | 5.53E+00 | 1.26E+00 |
| NM_006585 | CCT8 | 4.74E-13 | 4.11E-02 | 1.91E-11 | 3.65E-08 | 7.12E+00 | 4.95E+00 | 8.25E-02 |
| NM_012426 | SF3B3 | 8.64E-12 | 2.28E-09 | 2.23E-11 | 3.87E-01 | 6.10E+00 | 1.31E+00 | 3.59E-01 |
| NM_015317 | PUM2 | 7.39E-14 | 9.44E-02 | 5.10E-11 | 1.49E-08 | 6.97E+00 | 5.29E+00 | 8.18E-01 |
| NM_001007 | RPS4X | 9.82E-12 | 1.12E-02 | 6.08E-11 | 6.87E-07 | 1.02E+01 | 6.87E+00 | 1.20E+00 |
| NM_002392 | MDM2 | 1.88E-15 | 6.96E-01 | 1.23E-10 | 8.66E-11 | 9.46E+00 | 8.56E+00 | 2.44E+00 |
| NM_018838 | NDUFA12 | 2.73E-11 | 5.21E-04 | 1.31E-10 | 7.69E-05 | 8.96E+00 | 4.65E+00 | 1.79E-01 |
| NM_001013 | RPS9 | 9.80E-11 | 5.84E-07 | 2.31E-10 | 5.64E-02 | 7.26E+00 | 2.17E+00 | 1.61E-01 |

| | | | | | | | | |
|---|---|---|---|---|---|---|---|---|
| NM_012459 | TIMM8B | 1.86E-11 | 7.48E-11 | 2.91E-10 | 9.97E-01 | 5.50E+00 | 3.12E-01 | 1.91E-01 |
| NM_002815 | PSMD11 | 2.47E-14 | 8.67E-01 | 3.70E-10 | 5.96E-11 | 6.05E+00 | 5.52E+00 | 4.09E-01 |
| NM_001033044 | GLUL | 3.06E-10 | 6.28E-06 | 5.44E-10 | 1.83E-02 | 7.40E+00 | 2.53E+00 | 2.00E-02 |
| NM_017759 | INO80D | 3.26E-12 | 0.00E+00 | 1.17E-09 | 8.46E-01 | 5.12E+00 | 0.00E+00 | 4.41E-01 |
| NM_003079 | SMARCE1 | 5.71E-10 | 3.38E-03 | 1.38E-09 | 7.63E-05 | 6.68E+00 | 3.71E+00 | 1.43E-01 |
| NM_001144884 | SLC30A7 | 2.84E-12 | 7.43E-01 | 1.43E-09 | 1.07E-09 | 6.44E+00 | 5.70E+00 | 6.36E-01 |
| NM_002867 | RAB3B | 5.69E-11 | 3.99E-10 | 1.46E-09 | 9.99E-01 | 4.00E+00 | 8.55E+00 | 8.64E+00 |
| NM_004226 | STK17B | 1.34E-12 | 9.07E-01 | 2.06E-09 | 3.37E-10 | 6.49E+00 | 6.01E+00 | 9.78E-01 |
| NM_017952 | PTCD3 | 2.38E-10 | 3.20E-08 | 2.25E-09 | 6.37E-01 | 6.80E+00 | 1.39E+00 | 5.07E-01 |
| NM_001011 | RPS7 | 5.52E-09 | 9.25E-05 | 1.10E-08 | 2.10E-02 | 7.18E+00 | 2.75E+00 | 1.59E-01 |
| NR_037676 | FRMD6-AS1 | 2.31E-09 | 1.13E-08 | 1.27E-08 | 9.74E-01 | 6.33E+00 | 1.08E+01 | 1.10E+01 |
| NM_000885 | ITGA4 | 5.39E-11 | 9.60E-01 | 1.80E-07 | 2.89E-08 | 5.33E+00 | 4.96E+00 | 3.76E-01 |
| NM_198282 | TMEM173 | 6.47E-09 | 4.43E-08 | 1.97E-07 | 1.00E+00 | 5.92E+00 | 5.93E-01 | 5.84E-01 |
| NR_027378 | UG0898H09 | 3.51E-08 | 2.77E-07 | 2.21E-07 | 9.65E-01 | 3.58E+00 | 9.05E+00 | 9.43E+00 |
| NM_173084 | TRIM59 | 3.07E-11 | 6.99E-01 | 2.82E-06 | 6.19E-10 | 7.76E+00 | 8.73E+00 | 2.45E+00 |

923

924

925 **Supplementary Table 9.** Differentially expressed genes distinguishing cells cultured on laminin

926 vs PDMS and between apparent laminin subgroups in samples 1 and 2.

| | | | **Mean Expression (TPM)** | | | **StDev** | | | **SEM** | | |
|---|---|---|---|---|---|---|---|---|---|---|---|
| **transcript_id** | **Description** | **gene_id** | **Ln** | **Ln2** | **PDMS** | **Ln** | **Ln2** | **PDMS** | **Ln** | **Ln2** | **PDMS** |
| NM_001114380 | Integrin αL | ITGAL | 35.6 | 31.8 | 0.0 | 85.0 | 32.8 | 0.0 | 21.9 | 6.3 | 0.0 |
| NM_033668 | Integrin β1 | ITGB1 | 58.1 | 16.6 | 6.6 | 92.0 | 86.5 | 29.3 | 23.8 | 16.6 | 6.5 |
| NM_000885 | Integrin α4 | ITGA4 | 174.0 | 58.4 | 9.1 | 175.3 | 53.6 | 40.9 | 45.3 | 10.3 | 9.1 |
| NM_001136204 | | RCC2 | 364.8 | 75.5 | 0.0 | 353.2 | 168.7 | 0.0 | 91.2 | 32.5 | 0.0 |
| NM_001014794 | | ILK | 34.5 | 23.4 | 0.0 | 133.7 | 121.5 | 0.0 | 34.5 | 23.4 | 0.0 |
| NM_006720 | | ABLIM1 | 142.3 | 19.4 | 0.0 | 265.5 | 22.4 | 0.0 | 68.6 | 4.3 | 0.0 |
| NM_006633 | | IQGAP2 | 245.7 | 3.8 | 0.0 | 372.5 | 8.4 | 0.2 | 96.2 | 1.6 | 0.0 |
| NM_002872 | Small GTPase | RAC2 | 410.3 | 107.1 | 0.0 | 534.4 | 100.9 | 0.0 | 138.0 | 19.4 | 0.0 |
| NM_006289 | Talin 1 | TLN1 | 54.1 | 16.8 | 0.0 | 79.7 | 34.3 | 0.1 | 20.6 | 6.6 | 0.0 |
| NM_001079812 | mDia1 | DIAPH1 | 114.3 | 100.7 | 0.0 | 127.9 | 106.3 | 0.0 | 33.0 | 20.5 | 0.0 |
| NM_001244992 | Myosin phosphatase | PPP1R12A | 175.7 | 94.9 | 0.0 | 210.5 | 102.8 | 0.0 | 54.3 | 19.8 | 0.0 |
| NM_005406 | ROCK | ROCK1 | 51.6 | 141.7 | 6.7 | 106.5 | 707.6 | 30.2 | 27.5 | 136.2 | 6.7 |
| NR_033770 | ROCK Pseudogene | ROCK1P1 | 0.0 | 165.2 | 827.7 | 0.0 | 243.1 | 2261.0 | 0.0 | 46.8 | 505.6 |
| NM_005507 | Cofilin | CFL1 | 53.8 | 56.1 | 0.0 | 63.4 | 78.9 | 0.0 | 16.4 | 15.2 | 0.0 |
| NM_001201404 | WAVE | WASF2 | 628.7 | 1752.4 | 5365.9 | 604.9 | 3583.9 | 13059.5 | 156.2 | 689.7 | 2920.2 |
| NM_033546 | Myosin II | MYL12B | 444.7 | 8.9 | 0.3 | 826.3 | 35.1 | 1.4 | 213.3 | 6.8 | 0.3 |
| NM_079423 | Myosin II | MYL6 | 602.7 | 24.5 | 0.4 | 605.4 | 52.3 | 1.9 | 156.3 | 10.1 | 0.4 |
| NM_001012321 | "The Laminin Receptor" | RPSA | 789.1 | 237.8 | 57.1 | 763.2 | 334.3 | 255.2 | 197.1 | 64.3 | 57.1 |
| NM_001101 | β-actin | ACTB | 3840.3 | 1280.7 | 90.8 | 1543.1 | 971.9 | 406.1 | 398.4 | 187.1 | 90.8 |
| NM_001025109 | Differentiation marker | CD34 | 1730.0 | 125.0 | 21.9 | 1591.7 | 113.3 | 98.1 | 411.0 | 21.8 | 21.9 |
| NM_001791 | Small GTPase | CDC42 | 2936.8 | 770.5 | 33.2 | 2313.8 | 1166.3 | 148.3 | 597.4 | 224.4 | 33.2 |

| | | | | | | | | | | | |
|---|---|---|---|---|---|---|---|---|---|---|---|
| NM_005720 | Arp2/3 | ARPC1B | 179.3 | 40.4 | 0.0 | 324.9 | 142.0 | 0.0 | 83.9 | 27.3 | 0.0 |
| NM_005731 | Arp2/3 | ARPC2 | 2761.0 | 450.4 | 0.0 | 1406.5 | 640.8 | 0.0 | 363.2 | 123.3 | 0.0 |
| NM_152862 | Arp2/3 | ARPC2 | 239.8 | 6.6 | 0.0 | 338.1 | 34.4 | 0.0 | 87.3 | 6.6 | 0.0 |
| NM_001198780 | Arp2/3 | ARPC4 | 774.1 | 129.3 | 0.0 | 742.3 | 185.9 | 0.0 | 191.7 | 35.8 | 0.0 |
| NM_005717 | Arp2/3 | ARPC5 | 171.5 | 170.2 | 0.0 | 230.3 | 304.0 | 0.0 | 59.5 | 58.5 | 0.0 |

**Supplementary Table 10.** Genes identified by ANOVA from samples 1 and 2 distinguishing cells cultured on laminin vs PDMS and that are similar between apparent laminin subgroups indicating that they may represent a common set of distinguishing genes between PDMS and laminin culture. Average values represent Log2 transformed TPM.

| AccessionID | GeneID | Anova pValue | Ln2_vs_Ln pValue | PDMS_vs_Ln pValue | PDMS_vs_Ln2 pValue | Ln Average | Ln2 Average | PDMS Average |
|---|---|---|---|---|---|---|---|---|
| NM_006136 | CAPZA2 | 5.43E-17 | 1.000 | 0.00 | 0.00 | 6.444 | 6.420 | 0.000 |
| NM_001098210 | CTNNB1 | 1.97E-18 | 1.000 | 0.00 | 0.00 | 6.556 | 6.521 | 0.000 |
| NM_001081550 | THOC2 | 5.53E-22 | 0.998 | 0.00 | 0.00 | 5.538 | 5.622 | 0.000 |
| NM_001136555 | TLK1 | 5.97E-24 | 0.997 | 0.00 | 0.00 | 7.635 | 7.750 | 0.439 |
| NM_001145410 | NONO | 2.13E-28 | 0.983 | 0.00 | 0.00 | 7.271 | 7.450 | 0.000 |
| NM_015354 | NUP188 | 8.83E-17 | 0.976 | 0.00 | 0.00 | 5.633 | 5.384 | 0.000 |
| NM_001136479 | ANP32E | 2.60E-18 | 0.934 | 0.00 | 0.00 | 8.978 | 8.497 | 1.167 |
| NM_005028 | PIP4K2A | 1.27E-20 | 0.886 | 0.00 | 0.00 | 8.592 | 8.082 | 0.958 |
| NM_005004 | NDUFB8 | 5.20E-16 | 0.814 | 0.00 | 0.00 | 8.391 | 7.600 | 0.164 |
| NM_005722 | ACTR2 | 1.17E-17 | 0.807 | 0.00 | 0.00 | 7.028 | 6.432 | 0.553 |
| NM_001664 | RHOA | 3.57E-28 | 0.767 | 0.00 | 0.00 | 7.940 | 7.446 | 0.000 |
| NM_001415 | EIF2S3 | 8.97E-23 | 0.748 | 0.00 | 0.00 | 10.240 | 9.505 | 1.046 |
| NM_020801 | ARRDC3 | 9.59E-18 | 0.748 | 0.00 | 0.00 | 7.231 | 6.512 | 0.000 |
| NR_029435 | FLJ31306 | 3.04E-17 | 0.720 | 0.00 | 0.00 | 7.564 | 6.792 | 0.444 |
| NM_001130692 | PPP3CA | 3.05E-27 | 0.719 | 0.00 | 0.00 | 7.442 | 6.922 | 0.000 |
| NM_000314 | PTEN | 5.57E-31 | 0.715 | 0.00 | 0.00 | 8.811 | 8.290 | 0.385 |
| NM_006391 | IPO7 | 2.00E-17 | 0.706 | 0.00 | 0.00 | 5.715 | 5.101 | 0.000 |
| NM_003291 | TPP2 | 1.32E-16 | 0.673 | 0.00 | 0.00 | 5.396 | 4.765 | 0.000 |
| NM_013293 | TRA2A | 1.16E-20 | 0.665 | 0.00 | 0.00 | 8.219 | 7.409 | 0.000 |
| NM_006325 | RAN | 2.88E-17 | 0.660 | 0.00 | 0.00 | 7.817 | 6.915 | 0.000 |
| NM_004355 | CD74 | 5.62E-17 | 0.612 | 0.00 | 0.00 | 8.768 | 7.679 | 0.000 |
| NM_005839 | SRRM1 | 2.01E-16 | 0.598 | 0.00 | 0.00 | 6.973 | 6.139 | 0.546 |
| NM_001167582 | RBM6 | 1.91E-16 | 0.575 | 0.00 | 0.00 | 6.787 | 5.884 | 0.000 |
| NM_022731 | NUCKS1 | 5.01E-20 | 0.513 | 0.00 | 0.00 | 7.732 | 6.845 | 0.421 |
| NM_002032 | FTH1 | 1.20E-19 | 0.438 | 0.00 | 0.00 | 8.476 | 7.391 | 0.000 |
| NM_001244992 | PPP1R12A | 2.58E-17 | 0.426 | 0.00 | 0.00 | 6.267 | 5.327 | 0.000 |
| NM_017892 | PRPF40A | 2.87E-21 | 0.413 | 0.00 | 0.00 | 6.162 | 5.374 | 0.000 |
| NM_002798 | PSMB6 | 1.33E-17 | 0.410 | 0.00 | 0.00 | 8.461 | 7.188 | 0.000 |
| NM_015168 | ZC3H4 | 1.06E-19 | 0.398 | 0.00 | 0.00 | 5.715 | 4.921 | 0.000 |
| NM_002137 | HNRNPA2B1 | 5.84E-31 | 0.396 | 0.00 | 0.00 | 9.528 | 8.678 | 0.000 |
| NM_004308 | ARHGAP1 | 7.29E-18 | 0.393 | 0.00 | 0.00 | 6.970 | 5.936 | 0.000 |
| NM_175852 | TXLNA | 3.36E-25 | 0.373 | 0.00 | 0.00 | 8.222 | 7.303 | 0.000 |
| NM_001043318 | C14orf43 | 9.21E-22 | 0.330 | 0.00 | 0.00 | 8.595 | 7.499 | 0.860 |

| | | | | | | | | |
|---|---|---|---|---|---|---|---|---|
| NM_001248001 | SET | 9.26E-22 | 0.292 | 0.00 | 0.00 | 11.664 | 10.201 | 1.532 |
| NM_032983 | CASP2 | 2.71E-15 | 0.283 | 0.00 | 0.00 | 9.568 | 8.130 | 2.068 |
| NM_175854 | PAN3 | 6.20E-26 | 0.257 | 0.00 | 0.00 | 9.195 | 8.107 | 0.522 |
| NM_001031723 | DNAJB14 | 1.28E-20 | 0.255 | 0.00 | 0.00 | 7.793 | 6.628 | 0.435 |
| NM_018638 | ETNK1 | 1.78E-24 | 0.205 | 0.00 | 0.00 | 8.884 | 7.736 | 0.414 |
| NM_002796 | PSMB4 | 3.44E-42 | 0.196 | 0.00 | 0.00 | 9.931 | 9.186 | 0.000 |
| NM_001032284 | TMPO | 1.39E-21 | 0.189 | 0.00 | 0.00 | 7.964 | 6.764 | 0.468 |
| NM_001270661 | 6-Mar | 1.27E-20 | 0.177 | 0.00 | 0.00 | 7.112 | 5.900 | 0.000 |
| NM_001663 | ARF6 | 2.54E-19 | 0.171 | 0.00 | 0.00 | 7.309 | 5.986 | 0.027 |
| NM_134265 | WSB1 | 8.83E-14 | 0.170 | 0.00 | 0.00 | 6.809 | 5.254 | 0.000 |
| NM_000852 | GSTP1 | 2.80E-14 | 0.150 | 0.00 | 0.00 | 7.830 | 5.993 | 0.000 |
| NM_017664 | ANKRD10 | 1.91E-18 | 0.143 | 0.00 | 0.00 | 7.284 | 5.858 | 0.000 |
| NM_015934 | NOP58 | 3.92E-19 | 0.135 | 0.00 | 0.00 | 7.672 | 6.198 | 0.000 |
| NM_018011 | ARGLU1 | 1.02E-24 | 0.107 | 0.00 | 0.00 | 8.233 | 6.911 | 0.000 |
| NM_153810 | CACUL1 | 1.05E-15 | 0.085 | 0.00 | 0.00 | 7.249 | 5.623 | 0.335 |
| NM_003105 | SORL1 | 3.96E-17 | 0.079 | 0.00 | 0.00 | 6.523 | 5.018 | 0.000 |
| NR_003259 | GNAS | 3.35E-19 | 0.078 | 0.00 | 0.00 | 8.597 | 6.795 | 0.094 |
| NM_006386 | DDX17 | 4.99E-15 | 0.077 | 0.00 | 0.00 | 7.063 | 5.338 | 0.443 |
| NM_001008738 | FNIP1 | 1.02E-18 | 0.073 | 0.00 | 0.00 | 7.985 | 6.410 | 1.158 |

**Supplementary Table 11.** Genes identified by ANOVA distinguishing cells cultured on laminin vs PDMS and between apparent laminin subgroups from samples 1 and 2. Average values represent Log2 transformed TPM. All genes in this table have a PDMS average of 0, indicating that either the gene was not expressed, or it was low expressed and not detected by sequencing.

| AccessionID | GeneID | Anova pValue | Ln2_vs_Ln pValue | PDMS_vs_Ln pValue | PDMS_vs_Ln2 pValue | Ln Average | Ln2 Average | PDMS Average |
|---|---|---|---|---|---|---|---|---|
| NM_184041 | ALDOA | 4.93E-12 | 0.000 | 0.000 | 0.273 | 8.296 | 1.542 | 0.000 |
| NM_004343 | CALR | 2.36E-11 | 0.000 | 0.000 | 0.001 | 8.116 | 3.450 | 0.000 |
| NM_002803 | PSMC2 | 3.56E-13 | 0.000 | 0.000 | 1.000 | 5.113 | 0.000 | 0.000 |
| NM_001270 | CHD1 | 1.08E-12 | 0.000 | 0.000 | 0.941 | 4.905 | 0.287 | 0.000 |
| NM_003849 | SUCLG1 | 3.92E-13 | 0.000 | 0.000 | 1.000 | 5.578 | 0.000 | 0.000 |
| NM_002161 | IARS | 1.10E-11 | 0.000 | 0.000 | 0.000 | 7.195 | 3.165 | 0.000 |
| NM_002872 | RAC2 | 8.80E-14 | 0.174 | 0.000 | 0.000 | 6.868 | 5.267 | 0.000 |
| NM_006304 | SHFM1 | 1.57E-11 | 0.000 | 0.000 | 0.001 | 8.257 | 3.400 | 0.000 |
| NM_007278 | GABARAP | 1.69E-11 | 0.000 | 0.000 | 0.041 | 7.287 | 2.052 | 0.000 |
| NM_182810 | ATF4 | 1.04E-12 | 0.000 | 0.000 | 1.000 | 5.020 | 0.000 | 0.000 |
| NM_032233 | SETD3 | 2.97E-12 | 0.000 | 0.000 | 0.945 | 5.632 | 0.328 | 0.000 |
| NM_016480 | PAIP2 | 1.52E-16 | 0.978 | 0.000 | 0.000 | 6.837 | 7.151 | 0.000 |
| NM_139323 | YWHAB | 1.37E-14 | 0.917 | 0.000 | 0.000 | 6.281 | 5.813 | 0.000 |
| NM_014172 | PHPT1 | 3.96E-11 | 0.000 | 0.000 | 0.013 | 7.154 | 2.376 | 0.000 |
| NM_001018115 | FANCD2 | 8.40E-13 | 0.069 | 0.000 | 0.000 | 5.942 | 4.224 | 0.000 |
| NM_001001790 | TOMM5 | 3.56E-11 | 0.000 | 0.000 | 0.062 | 7.178 | 1.941 | 0.000 |
| NM_001024 | RPS21 | 4.43E-11 | 0.000 | 0.000 | 0.025 | 7.904 | 2.443 | 0.000 |
| NM_000992 | RPL29 | 4.77E-11 | 0.000 | 0.000 | 0.008 | 8.735 | 3.067 | 0.000 |
| NM_016293 | BIN2 | 8.32E-12 | 0.000 | 0.000 | 0.832 | 5.666 | 0.512 | 0.000 |
| NM_012255 | XRN2 | 2.01E-12 | 0.000 | 0.000 | 1.000 | 5.214 | 0.000 | 0.000 |
| NM_001131010 | SATB1 | 2.03E-12 | 0.000 | 0.000 | 1.000 | 4.892 | 0.000 | 0.000 |

| | | | | | | | | |
|---|---|---|---|---|---|---|---|---|
| NM_005450 | NOG | 1.11E-16 | 0.894 | 0.000 | 0.000 | 6.615 | 7.163 | 0.000 |
| NM_000999 | RPL38 | 2.06E-11 | 0.001 | 0.000 | 0.000 | 9.170 | 4.953 | 0.000 |
| NM_006802 | SF3A3 | 1.93E-11 | 0.000 | 0.000 | 0.925 | 5.794 | 0.387 | 0.000 |
| NM_012215 | MGEA5 | 9.61E-12 | 0.000 | 0.000 | 0.959 | 5.508 | 0.299 | 0.000 |
| NM_005005 | NDUFB9 | 1.03E-11 | 0.000 | 0.000 | 0.977 | 5.856 | 0.260 | 0.000 |
| NM_003753 | EIF3D | 1.53E-11 | 0.000 | 0.000 | 0.947 | 5.800 | 0.348 | 0.000 |
| NM_182692 | SRPK2 | 3.34E-11 | 0.000 | 0.000 | 0.744 | 6.043 | 0.672 | 0.000 |
| NM_005620 | S100A11 | 5.09E-11 | 0.002 | 0.000 | 0.000 | 8.445 | 4.623 | 0.000 |
| NM_019111 | HLA-DRA | 2.52E-12 | 0.154 | 0.000 | 0.000 | 7.633 | 5.665 | 0.000 |
| NM_002946 | RPA2 | 1.98E-11 | 0.000 | 0.000 | 0.968 | 6.329 | 0.321 | 0.000 |
| NM_006708 | GLO1 | 2.50E-11 | 0.000 | 0.000 | 0.936 | 5.556 | 0.362 | 0.000 |
| NM_001923 | DDB1 | 2.28E-11 | 0.000 | 0.000 | 0.963 | 5.151 | 0.276 | 0.000 |
| NM_001144772 | NSMAF | 3.61E-14 | 0.949 | 0.000 | 0.000 | 5.533 | 5.170 | 0.000 |
| NM_153280 | UBA1 | 1.27E-11 | 0.051 | 0.000 | 0.000 | 6.218 | 4.218 | 0.000 |
| NM_001126115 | TP53 | 6.63E-11 | 0.004 | 0.000 | 0.000 | 6.175 | 3.506 | 0.000 |
| NM_004231 | ATP6V1F | 2.64E-11 | 0.000 | 0.000 | 0.979 | 5.912 | 0.263 | 0.000 |
| NM_015965 | NDUFA13 | 1.16E-10 | 0.001 | 0.000 | 0.000 | 8.075 | 4.240 | 0.000 |
| NM_004446 | EPRS | 1.16E-10 | 0.000 | 0.000 | 0.545 | 5.862 | 0.880 | 0.000 |
| NM_003564 | TAGLN2 | 1.77E-11 | 0.000 | 0.000 | 1.000 | 4.990 | 0.000 | 0.000 |
| NM_003100 | SNX2 | 1.95E-11 | 0.000 | 0.000 | 1.000 | 4.976 | 0.000 | 0.000 |
| NM_006002 | UCHL3 | 4.77E-11 | 0.000 | 0.000 | 0.987 | 5.096 | 0.195 | 0.000 |
| NM_139207 | NAP1L1 | 2.33E-10 | 0.000 | 0.000 | 0.516 | 5.328 | 0.843 | 0.000 |
| NM_000108 | DLD | 2.79E-11 | 0.000 | 0.000 | 1.000 | 4.980 | 0.000 | 0.000 |
| NM_001021 | RPS17 | 1.35E-09 | 0.000 | 0.000 | 0.222 | 6.524 | 1.456 | 0.000 |
| NM_001199057 | RPS17L | 1.35E-09 | 0.000 | 0.000 | 0.222 | 6.524 | 1.456 | 0.000 |
| NM_006471 | MYL12A | 5.58E-12 | 0.281 | 0.000 | 0.000 | 6.831 | 5.282 | 0.000 |
| NM_006755 | TALDO1 | 1.45E-11 | 0.188 | 0.000 | 0.000 | 6.971 | 5.177 | 0.000 |
| NM_006009 | TUBA1A | 6.28E-10 | 0.001 | 0.000 | 0.001 | 6.989 | 3.380 | 0.000 |
| NM_000631 | NCF4 | 5.76E-11 | 0.000 | 0.000 | 1.000 | 5.148 | 0.000 | 0.000 |
| NM_001005 | RPS3 | 6.24E-09 | 0.000 | 0.000 | 0.005 | 7.305 | 3.009 | 0.000 |
| NM_003314 | TTC1 | 1.02E-10 | 0.000 | 0.000 | 1.000 | 4.991 | 0.000 | 0.000 |
| NM_005642 | TAF7 | 4.52E-12 | 0.884 | 0.000 | 0.000 | 6.133 | 5.548 | 0.000 |
| NM_002799 | PSMB7 | 1.79E-10 | 0.000 | 0.000 | 1.000 | 4.956 | 0.000 | 0.000 |
| NM_001398 | ECH1 | 7.97E-11 | 0.221 | 0.000 | 0.000 | 6.922 | 5.133 | 0.000 |
| NM_016478 | ZC3HC1 | 2.91E-10 | 0.000 | 0.000 | 1.000 | 4.737 | 0.000 | 0.000 |
| NM_015155 | LARP4B | 1.35E-15 | 0.406 | 0.000 | 0.000 | 4.736 | 5.734 | 0.000 |
| NM_006888 | CALM1 | 4.59E-15 | 0.168 | 0.000 | 0.000 | 4.997 | 6.417 | 0.000 |
| NM_001033 | RRM1 | 1.14E-11 | 0.854 | 0.000 | 0.000 | 5.674 | 5.050 | 0.000 |
| NM_003921 | BCL10 | 9.36E-11 | 0.652 | 0.000 | 0.000 | 5.114 | 4.275 | 0.000 |
| NM_001071 | TYMS | 4.44E-12 | 0.999 | 0.000 | 0.000 | 5.572 | 5.675 | 0.000 |
| NM_001079812 | DIAPH1 | 3.47E-16 | 0.045 | 0.000 | 0.000 | 4.292 | 5.979 | 0.000 |
| NM_001067 | TOP2A | 1.61E-16 | 0.024 | 0.000 | 0.000 | 4.950 | 7.090 | 0.000 |
| NM_006559 | KHDRBS1 | 1.98E-11 | 0.996 | 0.000 | 0.000 | 4.857 | 5.018 | 0.000 |
| NM_031992 | EIF4H | 5.13E-21 | 0.000 | 0.000 | 0.000 | 2.920 | 6.667 | 0.000 |
| NM_015975 | TAF9B | 4.88E-19 | 0.000 | 0.021 | 0.000 | 1.771 | 6.206 | 0.000 |
| NM_201599 | ZMYM3 | 1.68E-16 | 0.000 | 0.068 | 0.000 | 1.414 | 5.155 | 0.000 |
| NM_032525 | TUBB6 | 3.94E-23 | 0.000 | 0.210 | 0.000 | 1.109 | 6.853 | 0.000 |
| NM_177968 | PPM1B | 2.43E-19 | 0.000 | 0.223 | 0.000 | 0.988 | 5.416 | 0.000 |
| NM_001204199 | SRP19 | 6.80E-15 | 0.000 | 0.339 | 0.000 | 1.235 | 6.074 | 0.000 |
| NM_014117 | C16orf72 | 8.97E-20 | 0.000 | 0.467 | 0.000 | 0.742 | 5.289 | 0.000 |
| NM_006375 | ENOX2 | 1.41E-23 | 0.000 | 0.537 | 0.000 | 0.616 | 5.598 | 0.000 |
| NM_030962 | SBF2 | 9.11E-22 | 0.000 | 0.675 | 0.000 | 0.456 | 4.567 | 0.000 |
| NM_006315 | PCGF3 | 9.95E-13 | 0.000 | 0.703 | 0.000 | 0.713 | 4.992 | 0.000 |
| NM_001079685 | KIAA1191 | 1.72E-24 | 0.000 | 0.758 | 0.000 | 0.438 | 5.600 | 0.000 |
| NM_002098 | GUCA1B | 1.32E-08 | 0.000 | 0.777 | 0.000 | 0.701 | 4.283 | 0.000 |
| NR_027140 | TNFRSF10B | 9.90E-13 | 0.000 | 0.923 | 0.000 | 0.354 | 4.105 | 0.000 |
| NM_138957 | MAPK1 | 3.92E-19 | 0.000 | 0.951 | 0.000 | 0.313 | 5.807 | 0.000 |

| | | | | | | | | |
|---|---|---|---|---|---|---|---|---|
| NM_001145848 | PROM1 | 9.24E-08 | 0.000 | 0.991 | 0.000 | 0.252 | 4.193 | 0.000 |
| NM_000945 | PPP3R1 | 1.90E-13 | 0.000 | 0.996 | 0.000 | 0.130 | 4.421 | 0.000 |
| NM_145287 | ZNF519 | 1.06E-23 | 0.000 | 0.999 | 0.000 | 0.049 | 4.569 | 0.000 |
| NM_152695 | ZNF449 | 3.24E-15 | 0.000 | 1.000 | 0.000 | 0.000 | 4.284 | 0.000 |

939

940 **Supplementary Table 12.** Genes differentially expressed between MCSF-treated and untreated

941 cells in samples 1 and 2 for all ECM conditions.

| GeneID | Gene | P value for treated vs untreated S1, S2 | MCSF Treatment Effect - S1, S2 | P Value for treated vs untreated S3 | MCSF Treatment Effect - S3 |
|---|---|---|---|---|---|
| NM_000017 | ACADS | 1.16E-04 | Overexpressed | 1.02E-04 | Overexpressed |
| NM_016134 | CPQ | 4.68E-04 | Overexpressed | 1.25E-04 | Overexpressed |
| NM_032341 | DDI2 | 4.51E-06 | Overexpressed | 4.55E-05 | Overexpressed |
| NM_176815 | DHFRL1 | 1.51E-05 | Overexpressed | 5.58E-05 | Overexpressed |
| NM_001142725 | ERI2 | 1.49E-04 | Overexpressed | 8.02E-05 | Overexpressed |
| NM_001100910 | FAM72B | 2.18E-05 | Overexpressed | 6.74E-05 | Overexpressed |
| NM_001996 | FBLN1 | 2.15E-07 | Overexpressed | 1.42E-05 | Overexpressed |
| NM_005102 | FEZ2 | 4.11E-05 | Overexpressed | 2.14E-04 | Overexpressed |
| NR_039998 | LOC100506655 | 4.53E-04 | Overexpressed | 3.14E-03 | Overexpressed |
| NM_080822 | OVCA2 | 1.16E-10 | Overexpressed | 3.55E-04 | Overexpressed |
| NM_033288 | ZNF160 | 8.57E-06 | Overexpressed | 9.83E-03 | Overexpressed |

942

943 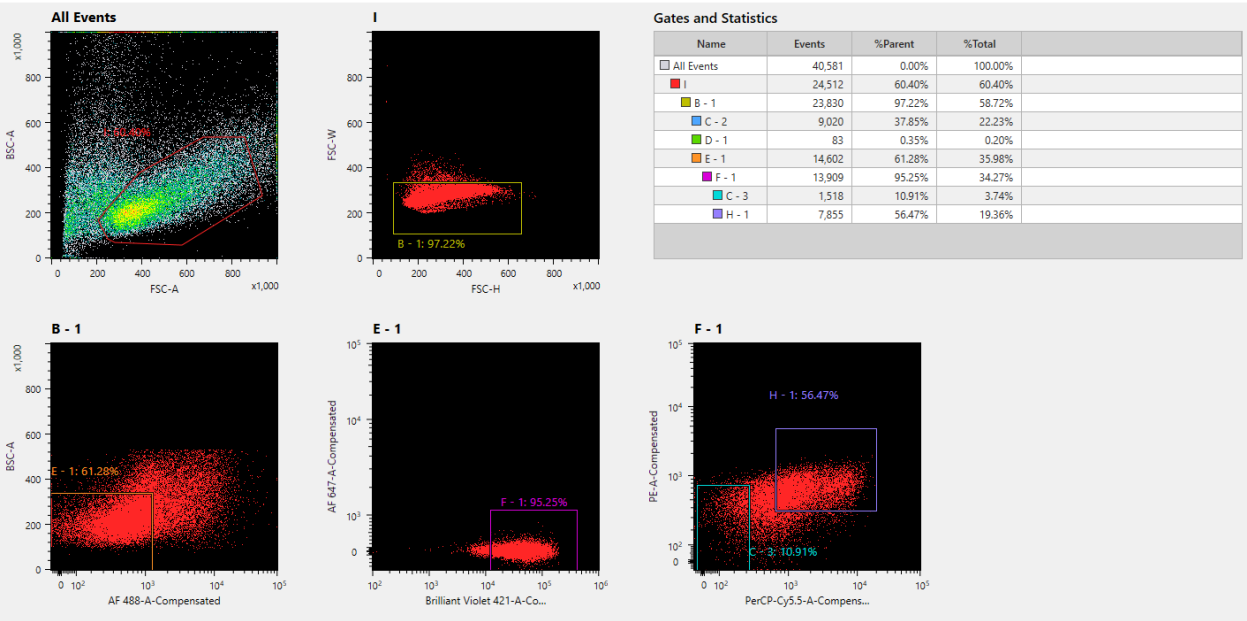


944 **Supplementary Figure 1**. FACS gating for sample 2. GMPs were isolated as described in the

945 methods section with staining as in **Supplementary Table 1** and **Supplementary Table 2**.

# 9. References


1. Murphy K, Weaver C. 2016. Janeway's immunobiology. Garland Science.

2. Crane GM, Jeffery E, Morrison SJ. 2017. Adult haematopoietic stem cell niches. Nat Rev Immunol advance online publication:. doi:10.1038/nri.2017.53. https://www.nature.com/nri/journal/vaop/ncurrent/abs/nri.2017.53.html.

3. Gattazzo F, Urciuolo A, Bonaldo P. 2014. Extracellular matrix: A dynamic microenvironment for stem cell niche. Biochimica et Biophysica Acta (BBA) - General Subjects 1840:2506-2519. doi:10.1016/j.bbagen.2014.01.010. http://www.sciencedirect.com/science/article/pii/S0304416514000129.

4. Ahmed M, French-Constant C. 2016. Extracellular Matrix Regulation of Stem Cell Behavior. Curr Stem Cell Rep 2:197-206. doi:10.1007/s40778-016-0056-2. https://search.proquest.com/docview/1880785295.

5. Notta F, Doulatov S, Laurenti E, Poeppl A, Jurisica I, Dick JE. 2011. Isolation of single human hematopoietic stem cells capable of long-term multilineage engraftment. Science 333:218-221.

6. Nerlov C, Drissen R, Buza-Vidas N, Woll P, Thongjuea S, Gambardella A, Giustacchini A, Jacobsen SE. 2016. Distinct myeloid progenitor differentiation pathways identified through single cell RNA sequencing. Experimental Hematology 44:S46. doi:10.1016/j.exphem.2016.06.058. http://www.ncbi.nlm.nih.gov/pmc/articles/PMC4972405/.

7. Markus G. Manz, Toshihiro Miyamoto, Koichi Akashi, Irving L. Weissman. 2002. Prospective Isolation of Human Clonogenic Common Myeloid Progenitors. Proceedings of the National Academy of Sciences of the United States of America 99:11872-11877. doi:10.1073/pnas.172384399. http://www.jstor.org/stable/3073131.

8. Nerlov C, Drissen R, Buza-Vidas N, Woll P, Thongjuea S, Gambardella A, Giustacchini A, Jacobsen SE. 2016. Distinct myeloid progenitor differentiation pathways identified through single cell RNA sequencing. Experimental Hematology 44:S46. doi:10.1016/j.exphem.2016.06.058. http://www.ncbi.nlm.nih.gov/pmc/articles/PMC4972405/.

9. Luc S, Buza-Vidas N, Jacobsen SEW. 2008. Delineating the cellular pathways of hematopoietic lineage commitment. Semin Immunol 20:213-220. doi:10.1016/j.smim.2008.07.005.

10. Ramalingam N, Fowler B, Szpankowski L, Leyrat AA, Hukari K, Maung MT, Yorza W, Norris M, Cesar C, Shuga J. 2016. Fluidic Logic Used in a Systems Approach to Enable Integrated Single-Cell Functional Analysis. Frontiers in Bioengineering and Biotechnology.

11. Wen L, Tang F. 2016. Single-cell sequencing in stem cell biology. Genome Biol 17:71.

12. Fang Ye, Wentao Huang, Guoji Guo. 2017. Studying hematopoiesis using single-cell technologies. Journal of Hematology & Oncology 10:1-12. doi:10.1186/s13045-017-0401-7. https://search.proquest.com/docview/1865011089.

13. Wilson NK, Kent DG, Buettner F, Shehata M, Macaulay IC, Calero-Nieto FJ, Sánchez Castillo M, Oedekoven CA, Diamanti E, Schulte R, Ponting CP, Voet T, Caldas C, Stingl J, Green AR, Theis FJ, Göttgens B. 2015. Combined Single-Cell Functional and Gene Expression Analysis Resolves Heterogeneity within Stem Cell Populations. Cell stem cell 16:712-724. doi:10.1016/j.stem.2015.04.004. http://www.ncbi.nlm.nih.gov/pubmed/26004780.

14. Wu J, Tzanakakis ES. 2013. Deconstructing stem cell population heterogeneity: single-cell analysis and modeling approaches. Biotechnol Adv 31:1047-1062. doi:10.1016/j.biotechadv.2013.09.001.

15. Kumari A, Golan K, Khatib-Massalha E, Kollet O, Lapidot T. 2017. Chapter Five-Mechanisms of Hematopoietic Stem and Progenitor Cells Bone Marrow Homing and Mobilization. Advances in Stem Cells and their Niches 1:85-121.

16. Aggarwal R, Lu J, J Pompili V, Das H. 2012. Hematopoietic stem cells: transcriptional regulation, ex vivo expansion and clinical application. Curr Mol Med 12:34-49.

17. Kanninen LK, Harjumki R, Peltoniemi P, Bogacheva MS, Salmi T, Porola P, Niklander J, Smutn T, Urtti A, Yliperttula ML. 2016. Laminin-511 and laminin-521-based matrices for efficient hepatic specification of human pluripotent stem cells. Biomaterials 103:86-100.

18. Muth CA, Steinl C, Klein G, Lee-Thedieck C. 2013. Regulation of hematopoietic stem cell behavior by the nanostructured presentation of extracellular matrix components. PloS one 8:e54778. doi:10.1371/journal.pone.0054778. http://www.ncbi.nlm.nih.gov/pubmed/23405094.

19. Parsons JT, Horwitz AR, Schwartz MA. 2010. Cell adhesion: integrating cytoskeletal dynamics and cellular tension. Nat Rev Mol Cell Biol 11:633-643. doi:10.1038/nrm2957.

20. Huttenlocher A, Horwitz AR. 2011. Integrins in cell migration. Cold Spring Harbor perspectives in biology 3:a005074. doi:10.1101/cshperspect.a005074. http://www.ncbi.nlm.nih.gov/pubmed/21885598.

21. Ananthakrishnan R, Ehrlicher A. 2007. The forces behind cell movement. International journal of biological sciences 3:303-317. http://www.ncbi.nlm.nih.gov/pubmed/17589565.

22. Hanna S, El-Sibai M. 2013. Signaling networks of Rho GTPases in cell motility. Cell Signal 25:1955-1961. doi:10.1016/j.cellsig.2013.04.009.

23. Carlier M, Shekhar S. 2017. Global treadmilling coordinates actin turnover and controls the size of actin networks. Nat Rev Mol Cell Biol 18:389-401. doi:10.1038/nrm.2016.172.

24. Krause M, Gautreau A. 2014. Steering cell migration: lamellipodium dynamics and the regulation of directional persistence. Nat Rev Mol Cell Biol 15:577-590. doi:10.1038/nrm3861. https://www.nature.com/nrm/journal/v15/n9/full/nrm3861.html.

25. Ridley AJ, Schwartz MA, Burridge K, Firtel RA, Ginsberg MH, Borisy G, Parsons JT, Horwitz AR. 2003. Cell migration: integrating signals from front to back. Science 302:1704-1709. doi:10.1126/science.1092053.

26. Luo B, Carman CV, Springer TA. 2007. Structural Basis of Integrin Regulation and Signaling. Annual Review of Immunology 25:619-647.

1025 doi:10.1146/annurev.immunol.25.022106.141618.
1026 http://www.ncbi.nlm.nih.gov/pubmed/17201681.

1027 27. Basu S, Hernandez I, Zogg M, Weiler H, Carlson KB, Kermani P. 2015. Physiologic
1028 Hematopoiesis Is Dependent on Stromal Expression of Laminin-γ1. Blood 126:3596.

1029 28. Mi H, Muruganujan A, Casagrande JT, Thomas PD. 2013. Large-scale gene function
1030 analysis with the PANTHER classification system. Nature protocols 8:1551-1566.

1031 29. Mi H, Huang X, Muruganujan A, Tang H, Mills C, Kang D, Thomas PD. 2016. PANTHER
1032 version 11: expanded annotation data from Gene Ontology and Reactome pathways, and data
1033 analysis tool enhancements. Nucleic Acids Res gkw1138.

1034 30. Thomas PD, Kejariwal A, Guo N, Mi H, Campbell MJ, Muruganujan A, Lazareva-Ulitsky B.
1035 2006. Applications for protein sequence–function evolution data: mRNA/protein expression
1036 analysis and coding SNP scoring tools. Nucleic Acids Res 34:W650.

1037 31. Gu Y, Kortesmaa J, Tryggvason K, Persson J, Ekblom P, Jacobsen S, Ekblom M. 2003.
1038 Laminin isoform–specific promotion of adhesion and migration of human bone marrow
1039 progenitor cells. Blood 101:877-885.

1040 32. Siler U, Seiffert M, Puch S, Richards A, Torok-Storb B, Mller CA, Sorokin L, Klein G.
1041 2000. Characterization and functional analysis of laminin isoforms in human bone marrow.
1042 Blood 96:4194-4203.

33. Jacquemet G, Morgan MR, Byron A, Humphries JD, Choi CK, Chen CS, Caswell PT, Humphries MJ. 2013. Rac1 is deactivated at integrin activation sites through an IQGAP1–filamin-A–RacGAP1 pathway. J Cell Sci 126:4121-4135.

34. Lapid K, Glait-Santar C, Gur-Cohen S, Canaani J, Kollet O, Lapidot T. 2012. Egress and mobilization of hematopoietic stem and progenitor cells: a dynamic multi-facet process. .

35. Humphries JD, Byron A, Bass MD, Craig SE, Pinney JW, Knight D, Humphries MJ. 2009. Proteomic analysis of integrin-associated complexes identifies RCC2 as a dual regulator of Rac1 and Arf6. Science signaling 2:ra51.

36. McCarty WJ, Prodanov L, Bale SS, Bhushan A, Jindal R, Yarmush ML, Usta OB. 2015. Layer-by-layer Collagen Deposition in Microfluidic Devices for Microtissue Stabilization. Journal of visualized experiments: JoVE .

37. Vallejos CA, Risso D, Scialdone A, Dudoit S, Marioni JC. 2017. Normalizing single-cell RNA sequencing data: challenges and opportunities. Nat Meth 14:565-571. doi:10.1038/nmeth.4292. http://www.nature.com/nmeth/journal/v14/n6/abs/nmeth.4292.html?foxtrotcallback=true.

38. Lun ATL, Bach K, Marioni JC. 2016. Pooling across cells to normalize single-cell RNA sequencing data with many zero counts. Genome Biol 17:75. doi:10.1186/s13059-016-0947-7.

1061 39. Thrasher AJ, Burns SO. 2010. WASP: a key immunological multitasker. Nat Rev Immunol
1062 10:182-192. doi:10.1038/nri2724.
1063 http://www.nature.com/nri/journal/v10/n3/full/nri2724.html.

1064 40. Montefusco MC, Merlo K, Bryan CD, Surks HK, Reis SE, Mendelsohn ME, Huggins GS.
1065 2010. Little ROCK is a ROCK1 pseudogene expressed in human smooth muscle cells. BMC
1066 Genet 11:22. doi:10.1186/1471-2156-11-22.

1067 41. Mohle R, Haas R, Hunstein W. 1993. Expression of adhesion molecules and c-kit on CD34
1068 hematopoietic progenitor cells: comparison of cytokine-mobilized blood stem cells with
1069 normal bone marrow and peripheral blood. J Hematother 2:483-489.

1070 42. Gangenahalli GU, Singh VK, Verma YK, Gupta P, Sharma RK, Chandra R, Luthra PM.
1071 2006. Hematopoietic stem cell antigen CD34: role in adhesion or homing. Stem cells and
1072 development 15:305-313.

1073 43. Nielsen JS, McNagny KM. 2008. Novel functions of the CD34 family. J Cell Sci 121:3683-
1074 3692.

1075 44. Luders J. 2016. The Microtubule Cytoskeleton: Organisation, Function and Role in Disease.
1076 Springer.

1077 45. Bardua M, Haftmann C, Fang Z, Buttgereit A, Mcgrath M, Westendorf K, Maschmeyer P,
1078 Radbruch H, Chang HD, Rajewsky N. 2016. A2. 22 Microrna-31 modulates the expression
1079 of mobility related genes and the motility of T helper 1 lymphocytes. Ann Rheum Dis
1080 75:A24.

46. Yan X, Zhu X. 2013. Branched F-actin as a negative regulator of cilia formation. Exp Cell Res 319:147-151.

47. Roof DJ, Hayes A, Adamian M, Chishti AH, Li T. 1997. Molecular characterization of abLIM, a novel actin-binding and double zinc finger protein. J Cell Biol 138:575-588.

48. Amici SA, Dunn WA, Murphy AJ, Adams NC, Gale NW, Valenzuela DM, Yancopoulos GD, Notterpek L. 2006. Peripheral myelin protein 22 is in complex with α6β4 integrin, and its absence alters the Schwann cell basal lamina. Journal of Neuroscience 26:1179-1189.

49. Ito T, Ikeda K, Tomita K, Yokoyama S. 2010. Interleukin-6 upregulates the expression of PMP22 in cultured rat Schwann cells via a JAK2-dependent pathway. Neurosci Lett 472:104-108.

50. Laura Di Blasio, Paolo A Gagliardi, Alberto Puliafito, Luca Primo. 2017. Serine/Threonine Kinase 3-Phosphoinositide-Dependent Protein Kinase-1 (PDK1) as a Key Regulator of Cell Migration and Cancer Dissemination. Cancers 9:25. doi:10.3390/cancers9030025. https://search.proquest.com/docview/1889020144.

51. Lachmann N, Ackermann M, Frenzel E, Liebhaber S, Brennig S, Happle C, Hoffmann D, Klimenkova O, Lüttge D, Buchegger T, Kühnel MP, Schambach A, Janciauskiene S, Figueiredo C, Hansen G, Skokowa J, Moritz T. 2015. Large-scale hematopoietic differentiation of human induced pluripotent stem cells provides granulocytes or macrophages for cell replacement therapies. Stem cell reports 4:282-296. doi:10.1016/j.stemcr.2015.01.005. http://www.ncbi.nlm.nih.gov/pubmed/25680479.

52. Pupa SM, Ménard S, Forti S, Tagliabue E. 2002. New insights into the role of extracellular matrix during tumor onset and progression. J Cell Physiol 192:259-267. doi:10.1002/jcp.10142.

# 10. Biography

Cassandra was born in Glens Falls, New York in 1989. She attended Rochester Institute of Technology in 2007-2008, then transferred to Cornell University where she completed an undergraduate degree in Biological Engineering in 2011. Her undergraduate research in Dr. Antje Baeumner's microfluidics lab was published after she graduated (dx.doi.org/10.1021/ac403417z).

It was at Cornell that she met her husband-to-be; when he was accepted to Stanford's PhD program in Applied Physics, they moved to California together.

In 2015 Cassie started a master's program in Biotechnology through Johns Hopkins University while continuing to work in the biotech industry in the San Francisco Bay area.